Similarity of Discrete Gilbert-Elliot and Polya Channel Models to Continuous Rayleigh Fading Channel Model

Prepared by Sun, Pen-Ting

Advisory by Prof. Po-Ning Chen

In Partial Fulfillment of the Requirements

For the Degree of
Master of Science

Department of Communications Engineering

National Chiao Tung University

Hsinchu, Taiwan 300, R.O.C.

E-mail: yoo@atm.cm.nctu.edu.tw

June, 2002

Abstract

In this thesis, the concept of channel similarity is explored by two different methodologies—an analytical methodology based on divergence, and an empirical methodology based on error free run matching. In the analytical methodology, we showed that divergences can serve as an index to channel similarity. We then proceeded to compare the resemblance between the Gilbert-Elliott and Polya channels, and obtained that for some very specific case, the two channels are not *similar* to each other. In the empirical methodology, we examined which of the two channel models, Gilbert-Elliott and Polya, is more suitable to approximate the binary-quantized simplification of a continuous multipath Rayleigh fading channel. In terms of the *EFR* quantitative index, we showed that the Gilbert-Elliott channel is a better approximation to the binary-quantized multipath Rayleigh fading channel than the Polya model. A side result is that among all Rayleigh fading channels examined, the Gilbert-Elliott channel is particularly suitable to represent a two-path Rayleigh fading channel.

Acknowledgements

This part is under construction....

Contents

List of Tables

List of Figures

Chapter 1

Introduction

When the transmission rate for wireless communication is prohibitively low, the channel is sufficiently modelled as an additive white Gaussian noise (AWGN) channel. After being sampled, the AWGN channel is transformed to a discrete-in-time additive Gaussian channel, for which the additive noise at the present time instance is not statistically affected by the noises of other time instances. This noise phenomenon is often termed as *memoryless*. The memoryless binary symmetric channel, which is usually used as a typical channel for evaluating the hard-decision performance of a coding scheme, can then be treated as a binary-quantized simplification of the memoryless discrete-in-time additive Gaussian channel.

As the transmission rate is getting higher due to the demand of simultaneous transmission of voice and data, the channel noise is no longer memoryless in time, which results in a channel that exhibits *memory*. Thus, the classical memoryless binary symmetric channel is no longer effective in characterizing the coding transmission behavior for such channels. A need for developing a new channel model that well approximates a true channel with memory is therefore arose.

Three well-known channel models with memory have already been proposed in the literature, i.e., *the Gilbert model* [6], *the Gilbert-Elliot model* [4] and *the Fritchman model* [5].

These three channel models are in fact variations of hidden Markov models or finite-state channel models. Due to their simplicity, these three channel models are extensively used in mathematical analysis and computer simulations.

In 1994, F. Alajaji and T. Fuja [1] re-visited a channel model with memory, which is called the *Polya model*, and they found that feedback can indeed increases its feedforward channel capacity. Originally, the Polya model was used to model the spread of a contagion. Alajaji and Fuja noticed that this model is apt to approximate those channels whose errors, once occur, will increase the probability of the future errors. This provides an alternative channel model with memory for use of computer evaluation of coding performance.

Recently, some European researchers adopted the Polya model for simulating their joint source-channel coding scheme [7]. They have raised the question that "Is the binary Polya model more suitable to be treated as a binary-quantized simplification of a discrete-in-time continuous channel such as Rayleigh than the Gilbert-type model?" Their question motivates our research on the similarity of the Polya and Gilbert-Elliot channels to the Rayleigh fading channel. We split our quest along this research line into two different methodologies, a methodology based on a mathematical exploration and a methodology based on computer simulations. Results respectively for each methodology will be presented in Chapters 2 and 3 in this thesis.

This rest of the thesis is organized as follows. In Chapter 2, we gives a formal definition of similarity between two channel models. Based on the definition, similarity between the Polya mode and Gilbert-Elliot model is derived. In Chapter 3, we pre-specifies a targeted multi-path Rayleigh fading channel model. We then test which of the two channel models, i.e., Polya and Gilbert-Elliot channels, is a better approximation of the targeted channel based on a quantitative indicator named *error free run* (EFR). Chapter 4 concludes our research.

Chapter 2

Channel Similarity: Analysis Based on On Divergence

In this chapter, we give the definition of similarity between two channel models, followed by the derivation of channel similarity between *the Gilbert-Elliott model* and *the Polya model*. We begin with a brief review of these channel models.

2.1 Gilbert-Elliott Model

The Gilbert-Elliott model is basically a hidden Markov chain in its nature.

A simple description of a hidden Markov chain can be given as follows. A Markov chain is a stochastic process with a countable state space. The Markov chain resides in one of the states at each time instance, and the probability of making a transition to another state is a (time-stationary) function of the present state. With a Markov chain process hidden behind, the statistics of the observation process of a hidden Markov chain is determined by the present state from its associated Markov chain process.

As shown in Fig. 2.1, the Gilbert-Elliott model is a two-state hidden Markov chain, in which the two states are denoted by G (good state) and B (bad state). The state transition probability satisfies $\Pr(B|G) = b$ and $\Pr(G|B) = g$. In each state, the Gilbert-Elliott model

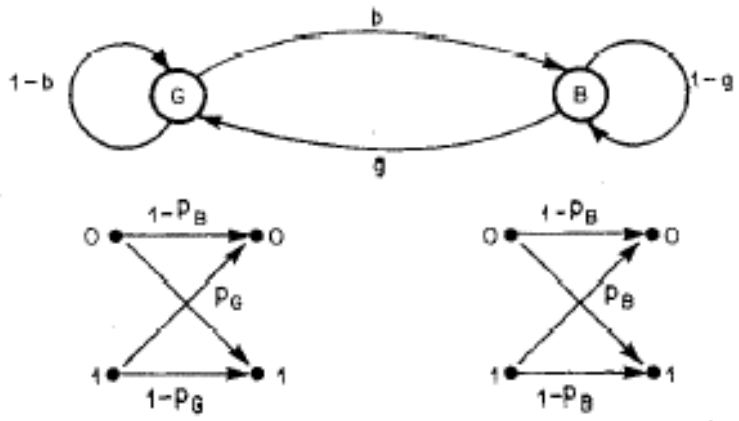

Figure 2.1: The State-Transition Diagram of the Gilbert-Elliott model[8]

acts exactly like a binary symmetric channel. The crossover probabilities for the good state and the bad state are denoted by P_G and P_B, respectively. Accordingly, the Gilbert-Elliott model is a model with four parameters, i.e., g, b, p_G and p_B.

Usually, p_G should be made relatively small to p_B as it is assumed that state G is a good and favored state. Also, g is usually small; hence, the bad state tends to persist, which emulates the *burst error state* in practical computation system. As long as one of g and b is positive, the Gilbert-Elliott channel model has memory. The state process for the Gilbert-Elliott model can be made stationary by assuming the initial state probability

$$\Pr(S_0 = G) = \frac{g}{g+b} \quad \text{and} \quad \Pr(S_0 = B) = \frac{b}{g+b}. \tag{2.1}$$

2.2 Polya Model

The Polya model is a binary additive communication channel with memory [1]. Specifically,

$$Y_i = X_i \oplus Z_i \qquad \text{for} \quad i = 1, 2, 3, ... \tag{2.2}$$

where the ith channel output Y_i is a modulo-2 sum of the ith channel input $X_i \in \{0,1\}$ and the ith noise symbol $Z_i \in \{0,1\}$. The input sequence $\{X_i\}_{i=1}^{\infty}$ and the noise sequence $\{Z_i\}_{i=1}^{\infty}$ are independent of each other. The error spread in the Polya model is similar to the spread of a contagious disease through a population, where the occurrence of an error in the present time increases the probability of error occurrence in the future. The binary noise sequence $\{Z_i\}_{i=1}^{\infty}$ is drawn as follows. An urn originally contains R red balls (sick persons) and S black balls (healthy persons). The balls are drawn successively from the urn. After each draw, $1+\Delta$ balls of the same color as was just drawn are returned to the urn. Then the noise sequence $\{Z_i\}_{i=1}^{\infty}$ is given by

$$Z_i = \begin{cases} 1, & \text{if the } i\text{th ball drawn is red} \\ 0, & \text{if the } i\text{th ball drawn is black.} \end{cases} \tag{2.3}$$

It can be seen from the above description that the Polya model is determined by three parameters, R, S and Δ. Hence, the number of parameters for the Polya model is less than that of the Gilbert-Elliott model.

Often, it is assumed that $\Delta > 0$, which reflects the contagion condition. Also, the number of red ball R is usually less than the number of black ball S initially. According to [1], the block transition probability of the Polya model is given by [1]

$$\begin{aligned} P(Y^n = y^n \mid X^n = x^n) &= \frac{[\rho(\rho+\delta)...(\rho+(d-1)\delta)][\sigma(\sigma+\delta)...(\sigma+(n-d-1)\delta)]}{(1+\delta)(1+2\delta)...(1+(n-1)\delta)} \\ &= \frac{\Gamma(1/\delta)\Gamma(\rho/\delta+d)\Gamma(\sigma/\delta+n-d)}{\Gamma(\rho/\delta)\Gamma(\sigma/\delta)\Gamma(1/\delta+n)}, \end{aligned} \tag{2.4}$$

where

$$\delta = \Delta/(R+S), \tag{2.5}$$

$$\rho = R/(R+S), \tag{2.6}$$

$$\sigma = 1-\rho = S/(R+S), \tag{2.7}$$

d is the Hamming distance between x^n and y^n, and $\Gamma(x) = \int_0^{\infty} t^{x-1}e^{-t}dt$, defined for $x > 0$, is the well-known Gamma function.

2.3 Channel Similarities

The quantitative index of our channel similarity definition is defined based on the output error probability due to a transmission scheme. Specifically, we presume that if two channel models are completely *similar*, then their resultant error probabilities due to the same transmission scheme should be the same. Also, a channel model can resemble or replace the other channel model, if for any model parameters chosen for the second channel model, there exists some model parameters for the first channel model such that the two channels yield the same error probability due to a transmission scheme. Based on these conceptual guideline, the similarity of the Gilbert-Elliott channel model and the Polya channel model will be derived; and in case the Polya channel model can replace the Gilbert-Elliott channel model, one can surely use the simpler three-parameter Polya channel in his/her simulations instead of the four-parameter Gilbert-Elliott channel model.

2.3.1 Preliminaries

Definition 2.1 (variational distance) *The variational distance between two distributions P_X and Q_X is defined as:*

$$\|P_X - Q_X\| \stackrel{\triangle}{=} \sum_{x \in \mathcal{X}} \left| P_X(x) - Q_X(x) \right|.$$

Definition 2.2 (expected conditional variational distance) *The expected conditional variational distance between two distributions $P_{X,Y}$ and $Q_{X,Y}$ is defined as:*

$$\begin{aligned} E\left[\, \|P_{Y|X} - Q_{Y|X}\| \, \middle| \, P_X \right] &\stackrel{\triangle}{=} \sum_{x \in \mathcal{X}} P_X(x) \cdot \left\| P_{Y|X}(\cdot|x) - Q_{Y|X}(\cdot|x) \right\| \\ &= \sum_{x \in \mathcal{X}} P_X(x) \cdot \left(\sum_{y \in \mathcal{Y}} \left| P_{Y|X}(y|x) - Q_{Y|X}(y|x) \right| \right). \end{aligned}$$

Definition 2.3 *An (f_n, g_n) data transmission code for channel input alphabet $\mathcal{X}^n$ and output alphabet $\mathcal{Y}^n$ consists of*

1. *M_n informational messages intended for transmission;*

2. *an encoding function*

$$f_n : \{1, 2, \ldots, M_n\} \to \mathcal{X}^n;$$

3. *a decoding function*

$$g_n : \mathcal{Y}^n \to \{1, 2, \ldots, M_n\},$$

which is (usually) a deterministic rule that assigns a guess to each possible received vector.

The channel inputs in $\{x^n \in \mathcal{X}^n \ : \ x^n = f_n(m) \text{ for some } 1 \leq m \leq M_n\}$ are the codewords of the data transmission code.

Definition 2.4 (probability of error) *The probability of error for an (f_n, g_n) code with a prior distribution over the codebook P_{X^n}, transmitted via channel $Q_{Y^n|X^n}$, is defined as*

$$P_e(f_n, Q_{Y^n|X^n}, g_n) = \sum_{i=1}^{M_n} P_{X^n}(f_n(i)) \cdot \lambda_i(f_n, Q_{Y^n|X^n}, g_n),$$

where

$$\lambda_i(f_n, Q_{Y^n|X^n}, g_n) \stackrel{\triangle}{=} \sum_{\left\{y^n \in \mathcal{Y}^n \ : \ g_n(y^n) \neq i\right\}} Q_{Y^n|X^n}(y^n | f_n(i)).$$

Furthermore,

$$P_e^*(f_n, Q_{Y^n|X^n}) \stackrel{\triangle}{=} \min_{g_n} P_e(f_n, Q_{Y^n|X^n}, g_n),$$

where the minimum probability of error corresponding to channel encoder $f_n(\cdot)$ and $P_{X^n} Q_{Y_n|X^n}$ is achieved by the MAP decoder.

Although the error probability is the performance index that a system designer concerns most, its derivation often much involves with the encoding function taken. Instead, we found that if the Kullback-Leiber divergence of the two channel statistics is small, the error probability difference for a transmission scheme over the two channels shall be smaller. Hence, we can actually measure the channel similarity in terms of the divergence of the two channel statistics. The theories on which the above arguments are based are introduced below.

Theorem 2.1 *Fix a channel encoder $f_n(\cdot)$, a distribution over the codebook P_{X^n} and a channel decoder $g_n(\cdot)$. For any two channels respectively defined through transition probabilities $P_{Y^n|X^n}$ and $Q_{Y^n|X^n}$,*

$$\left|P_e(f_n, P_{Y^n|X^n}, g_n) - P_e(f_n, Q_{Y^n|X^n}, g_n)\right| \leq \frac{1}{2} E\left[\, \left\|P_{Y^n|X^n} - Q_{Y^n|X^n}\right\| \,\middle|\, P_{X^n}\right].$$

Proof:

$$\begin{aligned}
& \left|\lambda_i(f_n, Q_{Y^n|X^n}, g_n) - \lambda_i(f_n, P_{Y^n|X^n}, g_n)\right| \\
= & \left| \sum_{\left\{y^n \in \mathcal{Y}^n \,:\, g_n(y^n) \neq i\right\}} \left[Q_{Y^n|X^n}(y^n|f_n(i)) - P_{Y^n|X^n}(y^n|f_n(i))\right] \right| \\
\leq & \sum_{\left\{y^n \in \mathcal{Y}^n \,:\, g_n(y^n) \neq i\right\}} \left|Q_{Y^n|X^n}(y^n|f_n(i)) - P_{Y^n|X^n}(y^n|f_n(i))\right| \\
\leq & \frac{1}{2} \left\|Q_{Y^n|X^n}(\cdot|f_n(i)) - P_{Y^n|X^n}(\cdot|f_n(i))\right\|.
\end{aligned}$$

Hence,

$$\begin{aligned}
& \left|P_e(f_n, Q_{Y^n|X^n}, g_n) - P_e(f_n, P_{Y^n|X^n}, g_n)\right| \\
= & \left|\sum_{i=1}^{M_n} P_{X^n}(f_n(i)) \left[\lambda_i(f_n, Q_{Y^n|X^n}, g_n) - \lambda_i(f_n, P_{Y^n|X^n}, g_n)\right]\right| \\
\leq & \sum_{i=1}^{M_n} P_{X^n}(f_n(i)) \left|\lambda_i(f_n, Q_{Y^n|X^n}, g_n) - \lambda_i(f_n, P_{Y^n|X^n}, g_n)\right| \\
\leq & \frac{1}{2}\sum_{i=1}^{M_n} P_{X^n}(f_n(i)) \left\|Q_{Y^n|X^n}(\cdot|f_n(i)) - P_{Y^n|X^n}(\cdot|f_n(i))\right\| \\
= & \frac{1}{2} E\left[\, \left\|P_{Y^n|X^n} - Q_{Y^n|X^n}\right\| \,\middle|\, P_{X^n}\right].
\end{aligned}$$

■

Lemma 2.1 *Fix $\varepsilon > 0$. If two real-valued functions, $h_1(x)$ and $h_2(x)$, satisfy*

$$|h_1(x) - h_2(x)| \leq \varepsilon \quad \text{for every } x \in \Re,$$

then

$$\left|\min_{x\in\Re} h_1(x) - \min_{x\in\Re} h_2(x)\right| \leq \varepsilon.$$

Proof: For any $x \in \Re$,

$$h_1(x) - \varepsilon \leq h_2(x) \leq h_1(x) + \varepsilon.$$

Therefore, by taking minimum operation over $x \in \Re$, we obtain:

$$\min_{x\in\Re} h_1(x) - \varepsilon \leq \min_{x\in\Re} h_2(x) \leq \min_{x\in\Re} h_1(x) + \varepsilon.$$

■

Corollary 2.1 *Fix a channel encoder $f_n(\cdot)$ and a distribution over the codebook P_{X^n}. For any two channels respectively defined through transition probabilities $P_{Y^n|X^n}$ and $Q_{Y^n|X^n}$,*

$$\left|P_e^*(f_n, P_{Y^n|X^n}) - P_e^*(f_n, Q_{Y^n|X^n})\right| \leq \frac{1}{2} E\left[\, \left\|P_{Y^n|X^n} - Q_{Y^n|X^n}\right\| \,\middle|\, P_{X^n}\right].$$

Proof: This is an immediate consequence of Theorem 2.1 and Lemma 2.1. ■

Lemma 2.2 (variational distance and divergence *[3, Lemma 12.6.1]***)** *For any two distributions, P_X and Q_X,*

$$D(P_X\|Q_X) \geq \frac{1}{2}\cdot\|P_X - Q_X\|^2,$$

where $D(P_X\|Q_X)$ is the Kullback-Leibler divergence of P_X against Q_X.

By the above lemma, we can also obtain the next theorem.

Theorem 2.2 *Fix a channel encoder $f_n(\cdot)$ and a distribution over the codebook P_{X^n}. For any two channels respectively defined through transition probabilities $P_{Y^n|X^n}$ and $Q_{Y^n|X^n}$,*

$$\left|P_e^*(f_n, P_{Y^n|X^n}) - P_e^*(f_n, Q_{Y^n|X^n})\right| \leq \frac{1}{\sqrt{2}}\cdot D^{1/2}\left(P_{Y^n|X^n}\left\|Q_{Y^n|X^n}\right| P_{X^n}\right).$$

Proof:

$$\begin{aligned}
& \left|P_e^*(f_n, Q_{Y^n|X^n}) - P_e^*(f_n, P_{Y^n|X^n})\right| \\
\leq\ & \frac{1}{2}E\left[\ \left\|P_{Y^n|X^n} - Q_{Y^n|X^n}\right\|\ \middle|\ P_{X^n}\right] \\
=\ & \frac{1}{2}\sum_{i=1}^{M_n} P_{X^n}(f_n(i))\left\|Q_{Y^n|X^n}(\cdot|f_n(i)) - P_{Y^n|X^n}(\cdot|f_n(i))\right\| \\
\leq\ & \frac{\sqrt{2}}{2}\sum_{i=1}^{M_n} P_{X^n}(f_n(i))\sqrt{D(P_{Y^n|X^n}(\cdot|f_n(i))\|Q_{Y^n|X^n}(\cdot|f_n(i))} \\
\leq\ & \frac{\sqrt{2}}{2}\sqrt{\sum_{i=1}^{M_n} P_{X^n}(f_n(i))D(P_{Y^n|X^n}(\cdot|f_n(i))\|Q_{Y^n|X^n}(\cdot|f_n(i))} \qquad (2.8) \\
=\ & \frac{1}{\sqrt{2}}\cdot D^{1/2}\left(\ P_{Y^n|X^n}\right\|\ Q_{Y^n|X^n}\left|\ P_{X^n}\right.\right),
\end{aligned}$$

where (2.8) follows from Lyapounov's inequality [2, page 76], i.e., $E[U^{1/2}] \leq E^{1/2}[U]$. ■

2.3.2 Parameterized Channel Model

It can be observed that all channel models come with some parameters. For examples,

1. the memoryless BSC with one parameter ε;
2. the memoryless BEC with one parameter ρ;
3. the (binary) Gilbert-Elliott channel with parameters (b, g, p_B, p_G).

In the worst case, a binary channel can be characterized by $2^n \times 2^n$ parameters

$$[P_{Y^n|X^n}(y^n|x^n)] = \begin{bmatrix} p_{11} & p_{12} & \cdots & p_{1,2^n} \\ p_{21} & p_{22} & \cdots & p_{2,2^n} \\ \vdots & \vdots & & \vdots \\ p_{2^n,1} & p_{2^n,2} & \cdots & p_{2^n,2^n} \end{bmatrix}$$

Of course, the channel model in item 4 is not feasible in practical simulation, even in moderate n. So to speak, one can only employ the channel model with feasible formula and reasonable number of parameters when simulating the performance of a designed transmission scheme (code) over the channel model.

In the sequel, we will denote the channel statistics W^n (i.e., transition probability of channel output due to channel input), together with the model parameters $\vec{\lambda}$ associated with it, by $W^n(\vec{\lambda})$.

Now for a true channel W^n_{true} and a given computer-resolvable channel model $W^n(\vec{\lambda})$ with model parameter vector $\vec{\lambda}$, we say that the channel model "fits" to the true channel model, if there exists parameters $\vec{\lambda}$ such that the resultant bit error rates for a transmission scheme f_n under test due to W^n_{true} and $W^n(\vec{\lambda})$ are close, i.e.,

$$\min_{\vec{\lambda}} \left| P_e^*(f_n, W^n_{\text{true}}) - P_e^*(f_n, W^n(\vec{\lambda})) \right| < \varepsilon$$

for ε small, which is ensured by either

$$\min_{\vec{\lambda}} E\left[\|W^n_{\text{true}} - W^n(\vec{\lambda})\| \middle| X^n \right] < \varepsilon$$

or

$$\min_{\vec{\lambda}} D(W^n_{\text{true}} \| W^n(\vec{\lambda}) | X^n) < 2\varepsilon^2,$$

where X^n places equal weight on the codewords. Hence, $\min_{\vec{\lambda}} D(W^n_{\text{true}} \| W^n(\vec{\lambda}) | X^n)$ may be served as a good index of the "fitness" of the respective channel model to the true channel. However, in this case, the statistics of the true channel must be priori known.

We proceed to quatitatively define the channel resemblance. Suppose that there is a channel model $W_1^n(\vec{\lambda})$ that is widely accepted (because of its fitness to the true channel model). Then for any true channel, people would find a good estimate of the model parameter $\vec{\lambda}$ to the true channel, and simulate their designed transmission schemes over the channel model with the estimated $\vec{\lambda}$. In case a person proposes another channel model $W_2^n(\vec{\rho})$ with, say, less complexity. If the person can also show that for any $\vec{\lambda}$ satisfying $\left| P_e^*(f_n, W^n_{\text{true}}) - P_e^*(f_n, W_1^n(\vec{\lambda})) \right| < \gamma$,

$$\min_{\vec{\rho}} \left| P_e^*(f_n, W_1^n(\vec{\lambda})) - P_e^*(f_n, W_2^n(\vec{\rho})) \right| < \varepsilon \tag{2.9}$$

for some $\varepsilon > 0$ fixed, then

$$\min_{\vec{\rho}} |P_e^*(f_n, W^n_{\text{true}}) - P_e^*(f_n, W_2^n(\vec{\rho}))| < \varepsilon + \gamma.$$

The above result can be interpreted as follows. Since $W^n(\vec{\lambda})$ is believed to be a good model, γ should be small (at last for one proper choice of $\vec{\lambda}$). If $W_2^n(\vec{\rho})$ is shown to be close to $W_1^n(\vec{\lambda})$, i.e., ε is small, then $W_2^n(\vec{\rho})$ is $(\varepsilon + \gamma)$-close to the true channel. Consequently, (2.9) can be served as a guideline for how "good" the model $W_2^n(\vec{\rho})$ can resemble (or replace) the model $W_1^n(\vec{\lambda})$. In extreme case, if model $W_2^n(\vec{\rho})$ can completely resemble model $W_1^n(\vec{\lambda})$ (i.e., the ε in (2.9) can be made arbitrarily small) and its number of model parameters is smaller (or has less complexity), then one can surely use the less complex model in his simulations.

Note that "model $W_2^n(\vec{\rho})$ well-resembles model $W_1^n(\vec{\lambda})$ in the sense of (2.9)" does not necessarily implies "model $W_1^n(\vec{\rho})$ well-resembles model $W_2^n(\vec{\lambda})$ in the sense of (2.9)." In

other words, the resultant implication is not symmetric.

Based on the above discussions, we may define the "resembility" of model $W_2^n(\vec{\rho})$ to model $W_1^n(\vec{\lambda})$ as the quantity:

$$\max_{\vec{\lambda}} \min_{\vec{\rho}} \left| P_e^*(f_n, W_1^n(\vec{\lambda})) - P_e^*(f_n, W_2^n(\vec{\rho})) \right|. \tag{2.10}$$

Similarly, the "resembility" of model $W_1^n(\vec{\lambda})$ to model $W_2^n(\vec{\rho})$ is:

$$\max_{\vec{\rho}} \min_{\vec{\lambda}} \left| P_e^*(f_n, W_1^n(\vec{\lambda})) - P_e^*(f_n, W_2^n(\vec{\rho})) \right|.$$

Comparison of the two quantities may serve as a guide of channel model "superiority."

Again, we can replace the condition in (2.10) by one defined through conditional divergence, i.e.,

$$\max_{\vec{\lambda}} \min_{\vec{\rho}} D(W_1^n(\vec{\lambda}))\|W_2^n(\vec{\rho}))|X^n). \tag{2.11}$$

In the next subsection, we will try to derive a close form formula for (2.11), where model $W_1^n(\vec{\lambda})$ is the Gilbert-Elliott model, and model $W_2^n(\vec{\rho})$ is the Polya model. The quantity indicates that how well the Polya model resembles the Gilbert-Elliott model.

2.3.3 Resemblance of Gilbert-Elliott and Polya models

The Gilbert-Elliott and Polya models can be expressed as

$$Y_i = X_i \oplus Z_i \quad \text{and} \quad Y_i = X_i \oplus \tilde{Z}_i,$$

where $Z^n = (Z_1, Z_2, \ldots, Z_n)$ and $\tilde{Z}^n = (\tilde{Z}_1, \tilde{Z}_2, \ldots, \tilde{Z}_n)$ are the corresponding Gilbert-Elliott and Polya urn drawing sequences, respectively. A known consequence of the additive binary channel with independence between channel input and noise sequences is that

$$P_{Y^n|X^n}(y^n|x^n) = P_{Z^n}(x^n \oplus y^n)$$

for any additive binary noise sequence Z^n. We can therefore re-write the divergence between the Gilbert-Elliott model and the Polya model as

$$D(W_1^n(\vec{\lambda})||W_2^n(\vec{\rho})|X_n) \;=\; E_{Z^n}\left[\log\frac{P_{Z^n}}{P_{\tilde{Z}^n}}\right] = E_{Z^n}\left[\log P_{Z^n}\right] - E_{Z^n}\left[\log P_{\tilde{Z}^n}\right].$$

It thus suffices to determine $E_{Z^n}\left[\log P_{Z^n}\right]$ and $E_{Z^n}\left[\log P_{\tilde{Z}^n}\right]$.

Denote by $S^n = (S_1, S_2, \ldots, S_n) \in \{G, B\}^n$ the states of the Gilbert-Elliott noise process Z^n. We then obtain

$$\begin{aligned}
E_{Z^n}\left[\log P_{Z^n}\right] &= E\left[E_{Z^n}\left[\log P_{Z^n}\middle|\, S^n\right]\right] \\
&= \sum_{s^n\in\{G,B\}^n} P_{S^n}(s^n) E_{Z^n}\left[\log P_{Z^n}\middle|\, S^n = s^n\right] \\
&= \sum_{s^n\in\{G,B\}^n} P_{S^n}(s^n) \sum_{i=1}^{n} E_{Z_i}\left[\log P_{Z_i}|S_i = s_i\right] \\
&= -\sum_{s^n\in\{G,B\}^n} P_{S^n}(s^n)\left[\ell_G(s^n)\cdot H_b(P_G) + (n-\ell_G(s^n))H_b(P_B)\right] \\
&= -\sum_{k=0}^{n}\left[k\cdot H_b(P_G) + (n-k)H_b(P_B)\right]\Pr\{\ell_G(S^n) = k\},
\end{aligned}$$

where $\ell_G(s^n)$ is the number of $s_i = G$ for $1 \le i \le n$, and $H_b(x) = -x\log(x) - (1-x)\log(1-x)$ is the binary Entropy function.

On the other hand, according to the Polya noise distribution given in (2.4),

$$\begin{aligned}
\frac{1}{n}E_{Z^n}\left[\log P_{\tilde{Z}^n}\right] &= \frac{1}{n}E_{Z^n}\left[\log\frac{\Gamma(1/\delta)\Gamma(\rho/\delta+d)\Gamma(\sigma/\delta+n-d)}{\Gamma(\rho/\delta)\Gamma(\sigma/\delta)\Gamma(1/\delta+n)}\right] \\
&= \frac{1}{n}\log\frac{\Gamma(1/\delta)}{\Gamma(\rho/\delta)\Gamma(\sigma/\delta)} + \frac{1}{n}E_{Z^n}\left[\log\frac{\Gamma(\rho/\delta+d)\Gamma(\sigma/\delta+n-d)}{\Gamma(1/\delta+n)}\right] \\
&= \frac{1}{n}\log\frac{\Gamma(1/\delta)}{\Gamma(\rho/\delta)\Gamma(\sigma/\delta)} + \frac{1}{n}E\left[E_{Z^n}\left[\log\frac{\Gamma(\rho/\delta+d)\Gamma(\sigma/\delta+n-d)}{\Gamma(1/\delta+n)}\middle|\, S^n\right]\right] \\
&= \frac{1}{n}\log\frac{\Gamma(1/\delta)}{\Gamma(\rho/\delta)\Gamma(\sigma/\delta)} + \frac{1}{n}\sum_{k=0}^{n}\Pr\{\ell_G(S^n) = k\} \\
&\quad\times\sum_{d_1=0}^{k}\sum_{d_2=0}^{n-k}\binom{k}{d_1}\binom{n-k}{d_2}p_G^{d_1}(1-p_G)^{k-d_1}p_B^{d_2}(1-p_B)^{n-k-d_2} \\
&\quad\times\log B(\rho/\delta+d_1+d_2, \sigma/\delta+n-d_1-d_2),
\end{aligned}$$

where $B(a,b) = \int_0^1 t^{a-1}(1-t)^{b-1}dt$ is the beta function. Consequently,

$$\begin{aligned}
&\lim_{n\to\infty}\frac{1}{n}D(W_1^n(\vec{\lambda})||W_2^n(\vec{\rho})|X_n)\\
=\ &-\lim_{n\to\infty}\sum_{k=0}^{n}\Pr\{\ell_G(S^n)=k\}\left[\frac{k}{n}\cdot H_b(P_G)+\left(1-\frac{k}{n}\right)H_b(P_B)\right]\\
&-\lim_{n\to\infty}\frac{1}{n}\sum_{k=0}^{n}\Pr\{\ell_G(S^n)=k\}\\
&\times\sum_{d_1=0}^{k}\sum_{d_2=0}^{n-k}\binom{k}{d_1}\binom{n-k}{d_2}p_G^{d_1}(1-p_G)^{k-d_1}p_B^{d_2}(1-p_B)^{n-k-d_2}\\
&\times\log B(\rho/\delta+d_1+d_2,\sigma/\delta+n-d_1-d_2),
\end{aligned}$$

provided the limit exists.

Here, as S^n is a first-order Markov process with $\Pr(S_{i+1}=G|S_i=B)=g$ and $\Pr(S_{i+1}=B|S_iG)=b$, the general solution for $\Pr\{\ell_G(S^n)=k\}$ may be complicated in its format. So we reduce to the simplest case, as a trial, of $g=b=1/2$ and $p_G=p_B=1/2$, which gives us $\Pr\{\ell_G(S^n)=k\}=\binom{n}{k}2^{-n}$ (this is exactly the binary symmetric channel with crossover probability 1/2). As a result,

$$\begin{aligned}
\frac{1}{n}E_{Z^n}\left[\log P_{Z^n}\right] &= -\sum_{k=0}^{n}\binom{n}{k}2^{-n}\left[\frac{k}{n}\cdot H_b(P_G)+\left(1-\frac{k}{n}\right)H_b(P_B)\right]\\
&= -H_b(p_G)\sum_{k=0}^{n}\frac{k}{n}\binom{n}{k}2^{-n}-H_b(p_B)\sum_{k=0}^{n}\frac{n-k}{n}\binom{n}{k}2^{-n}\\
&= -\frac{H_b(p_G)+H_b(P_B)}{2}=-\log(2).
\end{aligned}$$

In addition, by letting $R=S=\Delta$,

$$\begin{aligned}
\frac{1}{n}E_{Z^n}\left[\log P_{\tilde{Z}^n}\right] &= \frac{1}{n}\log\frac{\Gamma(2)}{\Gamma(1)\Gamma(1)}+\frac{1}{n}E_{Z^n}\left[\log\frac{\Gamma(1+d)\Gamma(1+n-d)}{\Gamma(2+n)}\right]\\
&= \frac{1}{n}\log\frac{1}{n}-\sum_{k=0}^{n}\binom{n}{k}2^{-n}\log\binom{n}{k}^{1/n}.
\end{aligned}$$

Hence, for this specific case,

$$\begin{aligned}
\lim_{n\to\infty}\frac{1}{n}D(W_1^n(\vec{\lambda})||W_2^n(\vec{\rho})|X_n) &= \lim_{n\to\infty}\sum_{k=0}^{n}\binom{n}{k}2^{-n}H_b(k/n)-\log(2)\\
&> \lim_{n\to\infty}2\sum_{k=0}^{\lfloor n/2\rfloor}\binom{n}{k}2^{-n}\cdot 2\log(2)\frac{k}{n}-\log(2)\\
&= \lim_{n\to\infty}2\log(2)\sum_{k=1}^{\lfloor n/2\rfloor}\binom{n-1}{k-1}2^{-(n-1)}-\log(2)=0.
\end{aligned}$$

Consequently, at least for this specific case, the Polya channel does not resemble the Gilbert-Elliott channel. But here, we did not optimize the model parameters of the Polya channel to fit the Gilbert-Elliott channel. Still, a lot of future work needs to be done along this research line.

Chapter 3

Channel Similarity: Analysis Based on Error Free Run

In this chapter, we assume that the true channel is a multi-path Rayleigh fading channel. This channel model is frequently used for simulations of wireless communication system. Notably, the assumed channel model is discrete in time but continuous in value. After binary quantization, the multi-path Rayleigh fading channel model can be transformed into a time-discrete binary channel. Our goal in this chapter is to examine which one of the Gilbert-Elliott and the Polya models is more "similar" to the binary-quantized multi-path Rayleigh fading channel.

Again, the concept behind channel similarity is that when two channels are similar, they should exhibit almost identical error behavior at the receiver end for the same transmission sequence. Here, instead of using the divergence of the transition probabilities of the channel models, which is an upper bound of the error difference, we introduce another quantitative indicator, the *error free run* (EFR). Based on this quantitative index, a channel model is similar to another channel model, if they give similar EFR due to the same transmission sequence. We can then examine the resemblance of the Gilbert-Elliott and the Polya models to the binary-quantized multi-path Rayleigh fading channel.

3.1 The Multi-Path Rayleigh Fading Channel Model

The impulse response of a simple multi-path Rayleigh fading channel model can be written as [10]:

$$h(\tau;t) = \sum_{n=0}^{L-1} \alpha_n(t) e^{-j2\pi f_c \tau_n} \delta(\tau - \tau_n), \tag{3.1}$$

where L is the number of channel paths, $\alpha_n(t)$ represents the time-variant aggregated attenuation corresponding path n with delay τ_n, and f_c is the carrier frequency. By employing some techniques, equation (3.1) can be simplified to:

$$h(\tau;t) = \sum_{n=0}^{L-1} \alpha_n(t) \delta(\tau - \tau_n). \tag{3.2}$$

Both (3.1) and (3.2) will be our targeted models for resemblance examination of the Gilbert-Elliott and the Polya models.

3.2 Error Free Run

In this section, we first define the error free run (EFR), and then derive the closed form expressions of the EFRs of the Gilbert-Elliott and the Polya models, respectively. The EFR of the binary-quantized multi-path Rayleigh fading channel will be obtained by computer simulations instead of analytical derivation.

To facilitate and simplify our analysis, we do not adopt the conventional EFR definition in [11], and define the *stationary EFR* specifically for our concerned hidden Markov channel model.

Definition 3.1 (Stationary Error Free Run for Hidden Markov) *Fix an additive binary channel, in which the binary output is the modulo-2 sum of the binary input and a binary noise sample. Suppose the binary noise samples are defined by a hidden Markov model. Then*

the stationary error free run *is defined as the probability of receiving at least consecutive m error free bits, given that an error has occurred, and is denoted by* $\mathrm{EFR}(m)$*, provided that the Markov state transition is stationary.*

From Definition 3.1, the EFR is the probability of receiving an error bit, followed by consecutive m correct bits. Next, we present the EFRs for the Gilbert-Elliott and Polya models.

⟨ `EFR of the Gilbert-Elliott model` ⟩

Following by the stationary state transition probability for the Gilbert-Elliott model, the stationary EFR of the Gilbert-Elliott model is given by:

$$\begin{aligned}\mathrm{EFR}_{\mathrm{GE}}(m) &= \Pr(S_0 = G)p_G(1-p_G)^m + \Pr(S_0 = B)p_B(1-p_B)^m \\ &= \left(\frac{g}{g+b}\right)p_G(1-p_G)^m + \left(\frac{b}{g+b}\right)p_B(1-p_B)^m.\end{aligned}$$

From the above formula, the complexity of $\mathrm{EFR}(m)$ increases exponentially as the error free run length m grows.

⟨ `EFR of the Polya model` ⟩

The Polya model can be viewed a hidden Markov model with infinite number of states, where the state is determined by the two parameters, R and S. The state transition probability can be described as:

$$P_{R_{j+1},S_{j+1}|R_j,S_j}(r_{j+1}, s_{j+1}|r_j, s_j) = \begin{cases} \dfrac{r_j}{r_j+s_j}, & \text{if } r_{j+1} = r_j + \Delta, s_{j+1} = s_j \\ \dfrac{s_j}{r_j+s_j}, & \text{if } r_{j+1} = r_j, s_{j+1} = s_j + \Delta. \end{cases}$$

Therefore, by taking $j = 1$ for simplicity, we obtain:

$$\begin{aligned}P_{R_2,S_2}(r_2, s_2) &= \sum_{r_1}\sum_{s_1} P_{R_1,S_1}(r_1, s_1)P_{R_2,S_2|R_1,S_1}(r_2, s_2|r_1, s_1) \\ &= P_{R_1,S_1}(r_2-\Delta, s_2)\frac{r_2-\Delta}{r_2+s_2-\Delta} + P_{R_1,S_1}(r_2, s_2-\Delta)\frac{s_2-\Delta}{r_2+s_2-\Delta}.\end{aligned}$$

It is then clear that the above Markov process cannot be made stationary. For example, taking $\Delta = 1$ yields

$$P_{R,S}(r,s) \;=\; P_{R,S}(r-1,s)\frac{r-1}{r+s-1} + P_{R,S}(r,s-1)\frac{s-1}{r+s-1},$$

provided $P_{R,S}(\cdot,\cdot)$ is the stationary state distribution, which implies that

$$P_{R,S}(r,s) = \frac{1}{r+s-1}P_{R,S}(1,1) \text{ for } r+s>1$$

Hence, the probability sum would equal infinity when $P_{R,S}(1,1) > 0$, and would be zero if $P_{R,S}(1,1) = 0$, where we reasonably and implicitly assume that the probability of $P_{R,S}(r,s) = 0$ for $r = 0$ or $s = 0$.

Hence, R and S can not be treated as state random variables if stationarity in *states* is required. In [1], Alajaji suggested to define the state as the total number of red balls drawn after n trials. With this new state definition, he showed that the Polya channel can be made stationary by treating R and S as pre-specified deterministic model parameters [1, pp. 2036]. Under his suggestion, we derive the EFR of the Polya model as follows.

$$\mathrm{EFR}_{\mathrm{Polya}}(m) \;=\; \left(\frac{R}{R+S}\right)\prod_{j=1}^{m}\left(\frac{S+(j-1)\Delta}{R+S+j\Delta}\right).$$

At the first glance, we may find the optimal model parameters for the Gilbert-Elliott and the Polya models, which best suit the simulated EFR from the binary-quantized Rayleigh fading channel model by means of "differentiation." As an example, under the total-squared error criterion, we may take the derivatives of $\mathrm{EFR}_{\mathrm{GE}}(m)$ with respect to g, b, p_G and p_B,

respectively, and yield:

$$\begin{aligned}
\frac{\partial}{\partial g}\sum_{j=1}^{m}\left[\mathrm{EFR}_{\mathrm{GE}}(j)-a_j\right]^2 &= \frac{2b}{(b+g)^2}\sum_{j=1}^{m}[P_G(1-P_G)^j-P_B(1-P_B)^j]\left[\mathrm{EFR}_{\mathrm{GE}}(j)-a_j\right] \\
&= 0 \\
\frac{\partial}{\partial b}\sum_{j=1}^{m}\left[\mathrm{EFR}_{\mathrm{GE}}(j)-a_j\right]^2 &= \frac{2g}{(b+g)^2}\sum_{j=1}^{m}[P_B(1-P_B)^j-P_G(1-P_G)^j]\left[\mathrm{EFR}_{\mathrm{GE}}(j)-a_j\right] \\
&= 0 \\
\frac{\partial}{\partial p_G}\sum_{j=1}^{m}\left[\mathrm{EFR}_{\mathrm{GE}}(j)-a_j\right]^2 &= \frac{g}{b+g}\sum_{j=1}^{m}(1-P_G)^{j-1}[1-(j+1)P_G]\left[\mathrm{EFR}_{\mathrm{GE}}(j)-a_j\right] \\
&= 0 \\
\frac{\partial}{\partial p_B}\sum_{j=1}^{m}\left[\mathrm{EFR}_{\mathrm{GE}}(j)-a_j\right]^2 &= \frac{b}{b+g}\sum_{j=1}^{m}(1-P_B)^{j-1}[1-(j+1)P_B]\left[\mathrm{EFR}_{\mathrm{GE}}(j)-a_j\right] \\
&= 0
\end{aligned}$$

where $a_1, a_2, \ldots, a_m$ are the simulated EFR values of the binary-quantized multi-path Rayleigh fading channel. Unfortunately, the above equations do not result a simple close-form solution. Therefore, the best-bit model parameters can only be selected though a simulation-based optimization.

Similarly, we tried to derive the optimal model parameters for the Polya channel through:

$$\begin{aligned}
\frac{\partial}{\partial R}\sum_{j=1}^{m}\left[\mathrm{EFR}_{\mathrm{Polya}}(j)-a_j\right]^2 &= 0 \\
\frac{\partial}{\partial S}\sum_{j=1}^{m}\left[\mathrm{EFR}_{\mathrm{Polya}}(j)-a_j\right]^2 &= 0 \\
\frac{\partial}{\partial \Delta}\sum_{j=1}^{m}\left[\mathrm{EFR}_{\mathrm{Polya}}(j)-a_j\right]^2 &= 0
\end{aligned}$$

Again, no close-form solution can be obtained; hence, a simulation-based parameter optimization is conducted.

3.3 Simulation System

Figure 3.1 illustrates the simulated multi-path Rayleigh fading channel model. 15 model parameters, such as the numbers of paths and system SNRs, that are used in our simulations are listed in Tab. 3.1. Additionally, we assume that conditions 1–12 are based on Eq. (3.2) in which no phase-rotate is observed, and conditions 13-15 are channels with random phase noise that is determined by the form of Eq. (3.1).

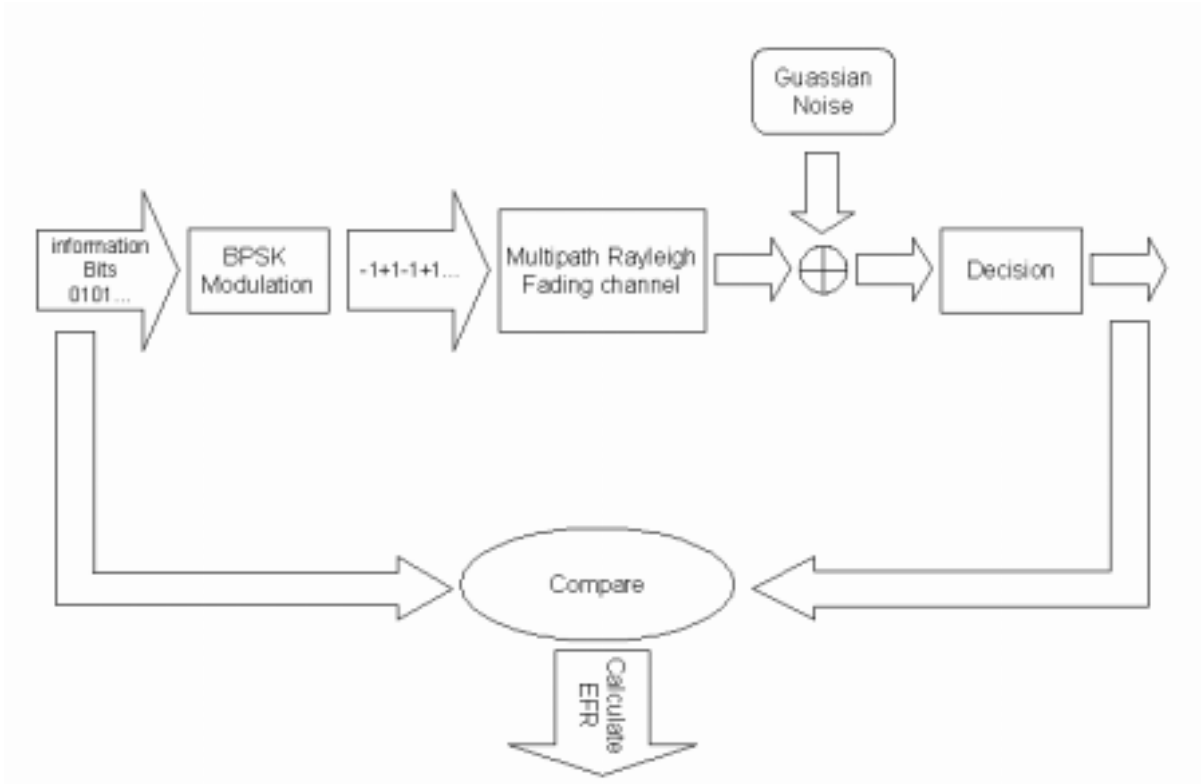

Figure 3.1: The system block diagram of the simulated multi-path Rayleigh fading channel model.

Other model parameters that affect the statistics of the multipath fading are chosen according to [9]. Specifically, exponential decay in path attenuation variance is assumed, and Jake's model is used for each path. Detailed setting for channel model is listed below.

Table 3.1: System parameters under different channel conditions.

Condition	Number of Path	SNR(dB)	Phase Rotate
1	1	5	X
2	1	10	X
3	1	15	X
4	2	5	X
5	2	10	X
6	2	15	X
7	6	5	X
8	6	10	X
9	6	15	X
10	10	5	X
11	10	10	X
12	10	15	X
13	2	5	O
14	2	10	O
15	2	15	O

T $\equiv$ BPSK symbol duration, which equals T_s
T_s $\equiv$ Sampling period at the receiver end
Doppler shift $=$ 8 Hz
Carrier frequency $=$ 2.4 GHz.

As aforementioned, we simulated the EFRs for the binary-quantized multi-path Rayleigh fading channel under 15 system conditions. For each condition, we obtain a set of model parameters for the Gilbert-Elliott and the Polya models through numerical optimization, subject to the total-square-error criterion. The resultant model parameters used in the simulations are listed in Tab. 17. The EFR fitting results for different channel conditions are plotted in Figs. 3.3–3.17, respectively.

3.4 Simulation Results

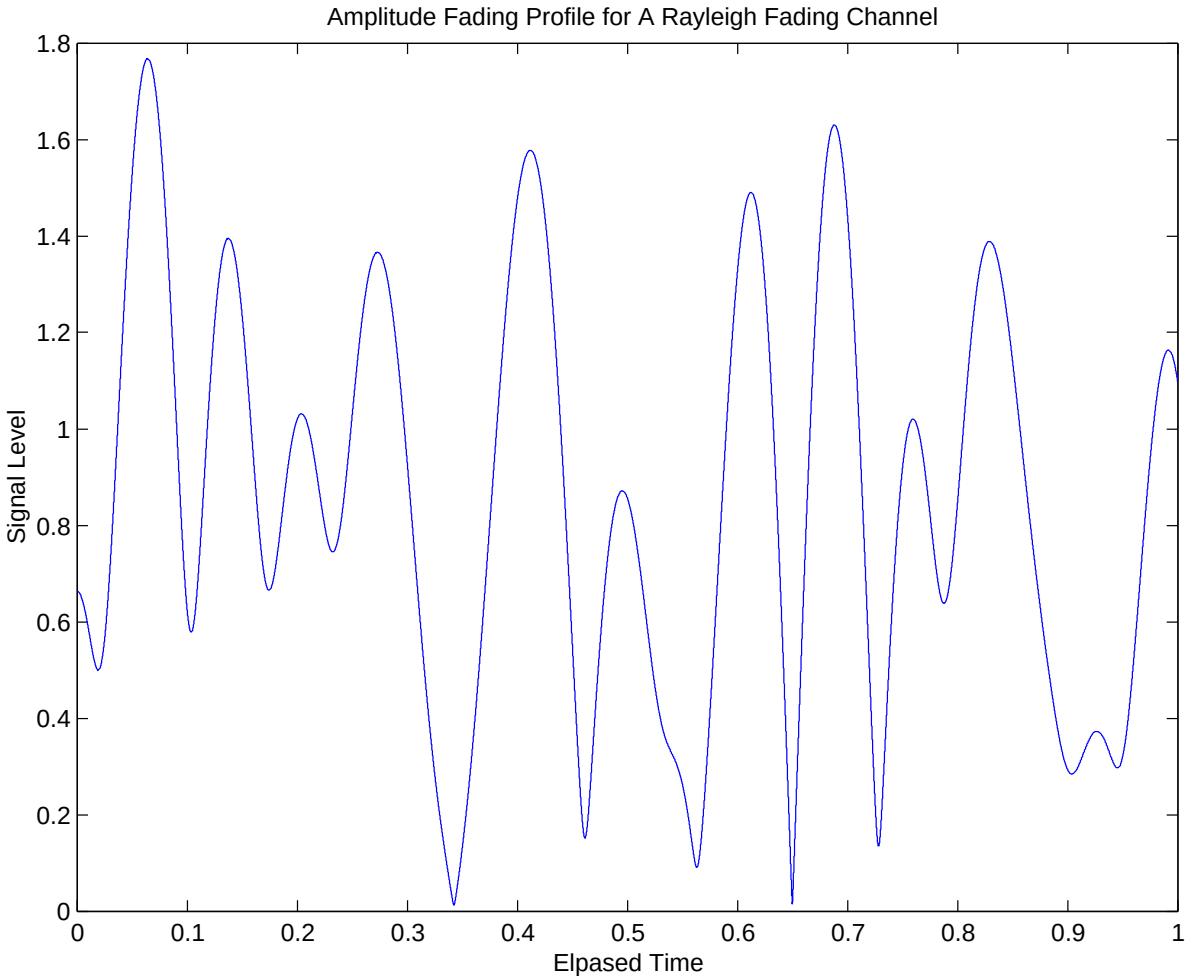

Figure 3.2: Amplitude fading profile obtained from Jake's model for the simulated Rayleigh fading channel.

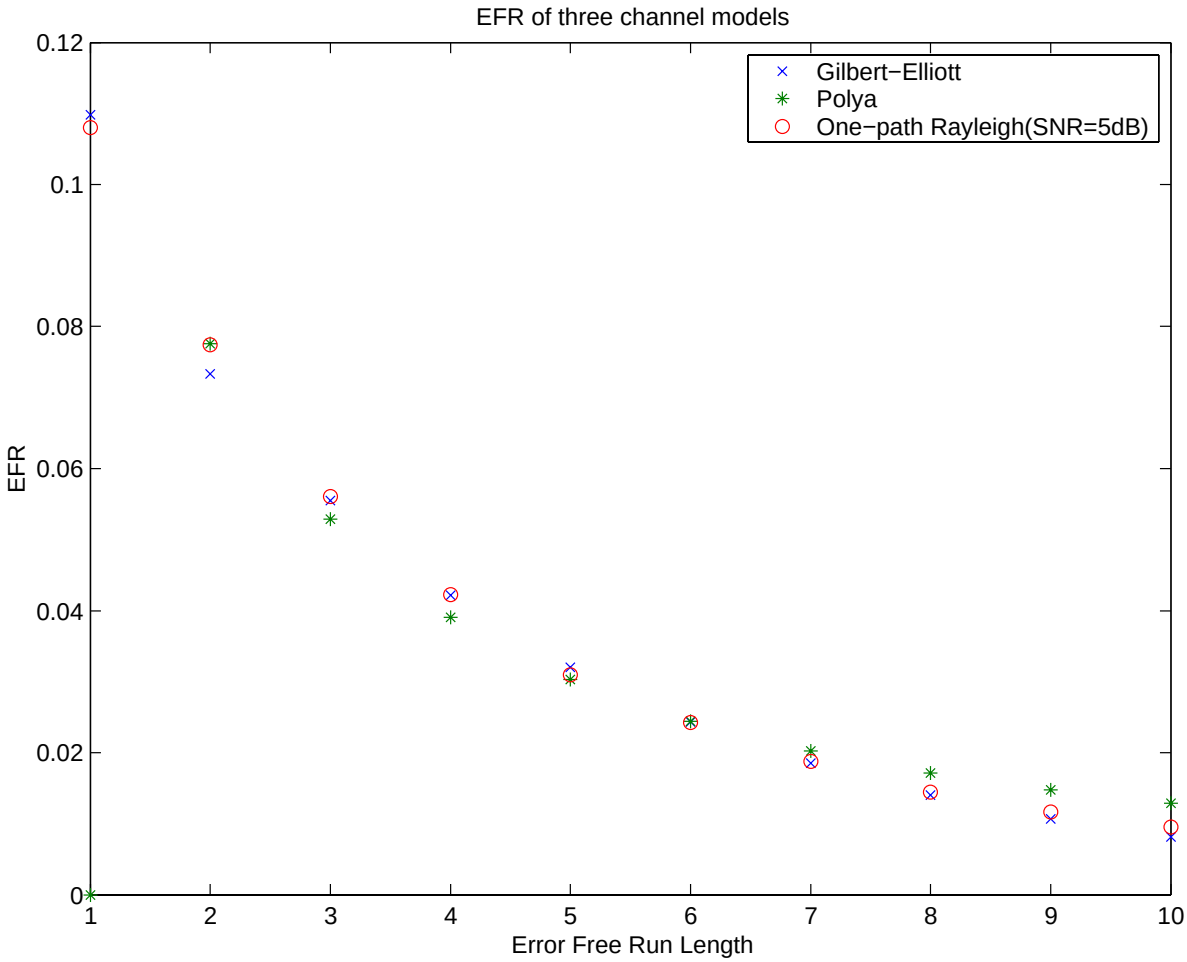

Figure 3.3: The Comparison Between the EFR of Three Models; condition 1

Table 3.2: The Total Difference of EFR Between Models; condition 1

Gilbert vs. Rayleigh	0.010790
Polya vs. Rayleigh	0.125852

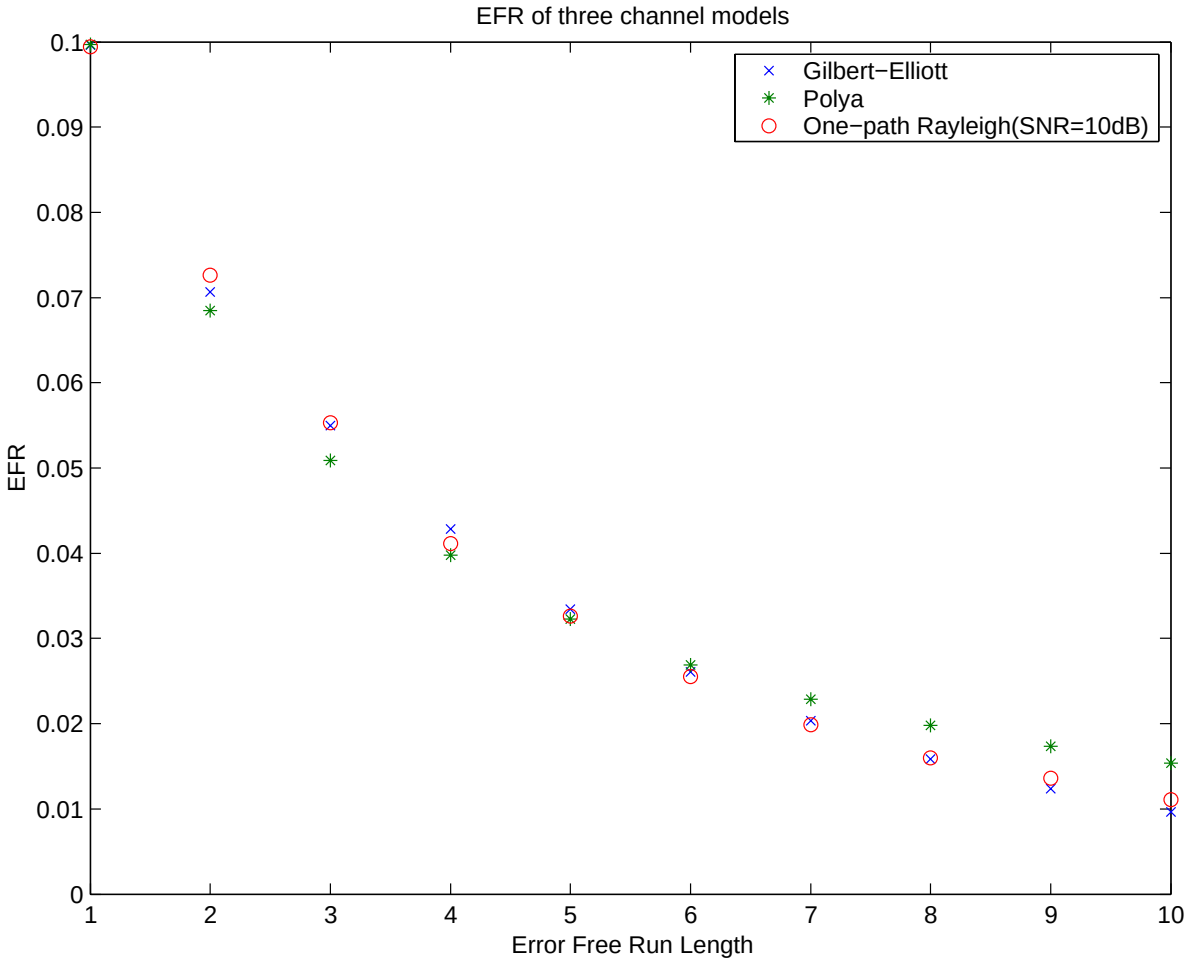

Figure 3.4: The Comparison Between the EFR of Three Models; condition 2

Table 3.3: The Total Difference of EFR Between Models; condition 2

Gilbert vs.Rayleigh	0.008870
Polya vs. Rayleigh	0.026915

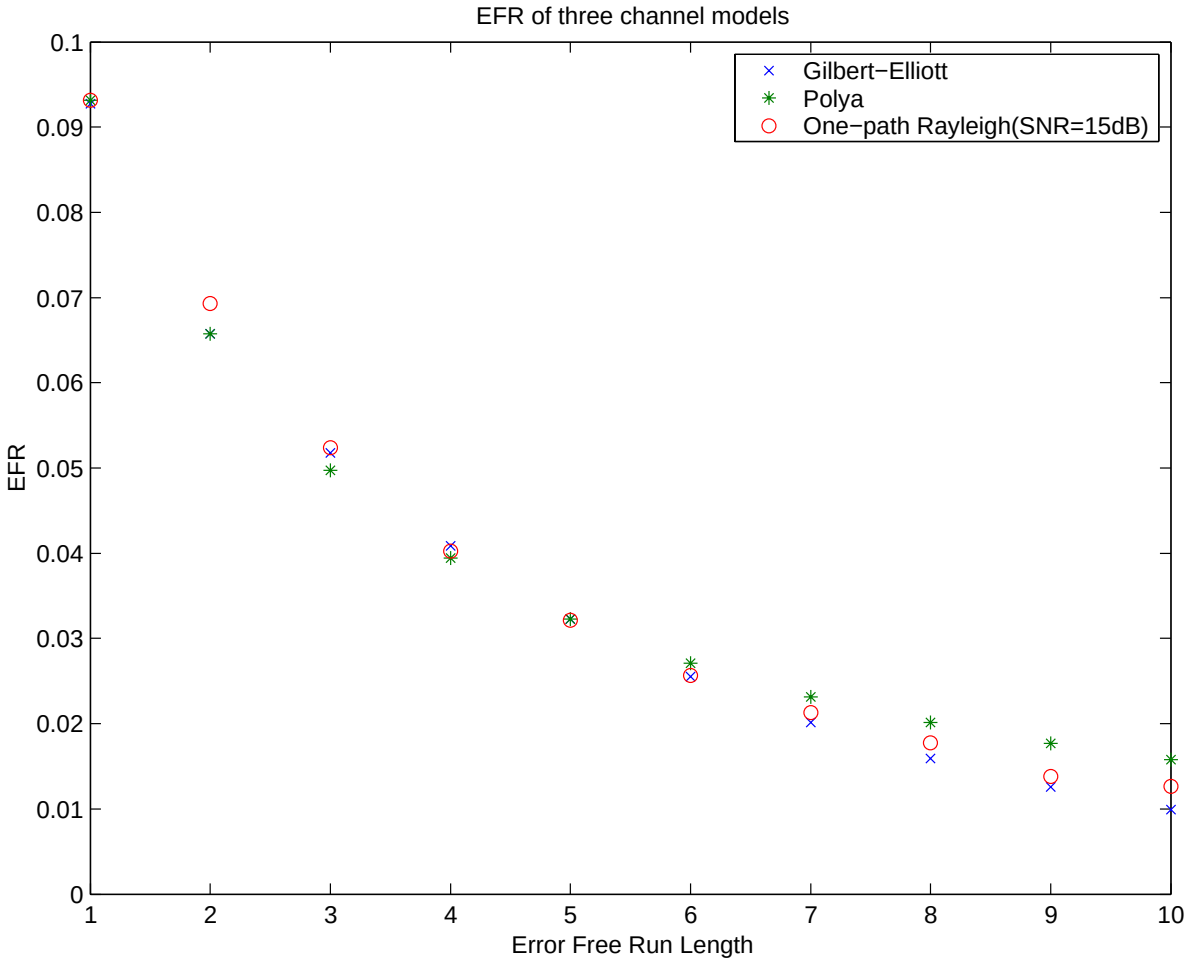

Figure 3.5: The Comparison Between the EFR of Three Models; condition 3

Table 3.4: The Total Difference of EFR Between Models; condition 3

Gilbert vs.Rayleigh	0.012391
Polya vs. Rayleigh	0.019862

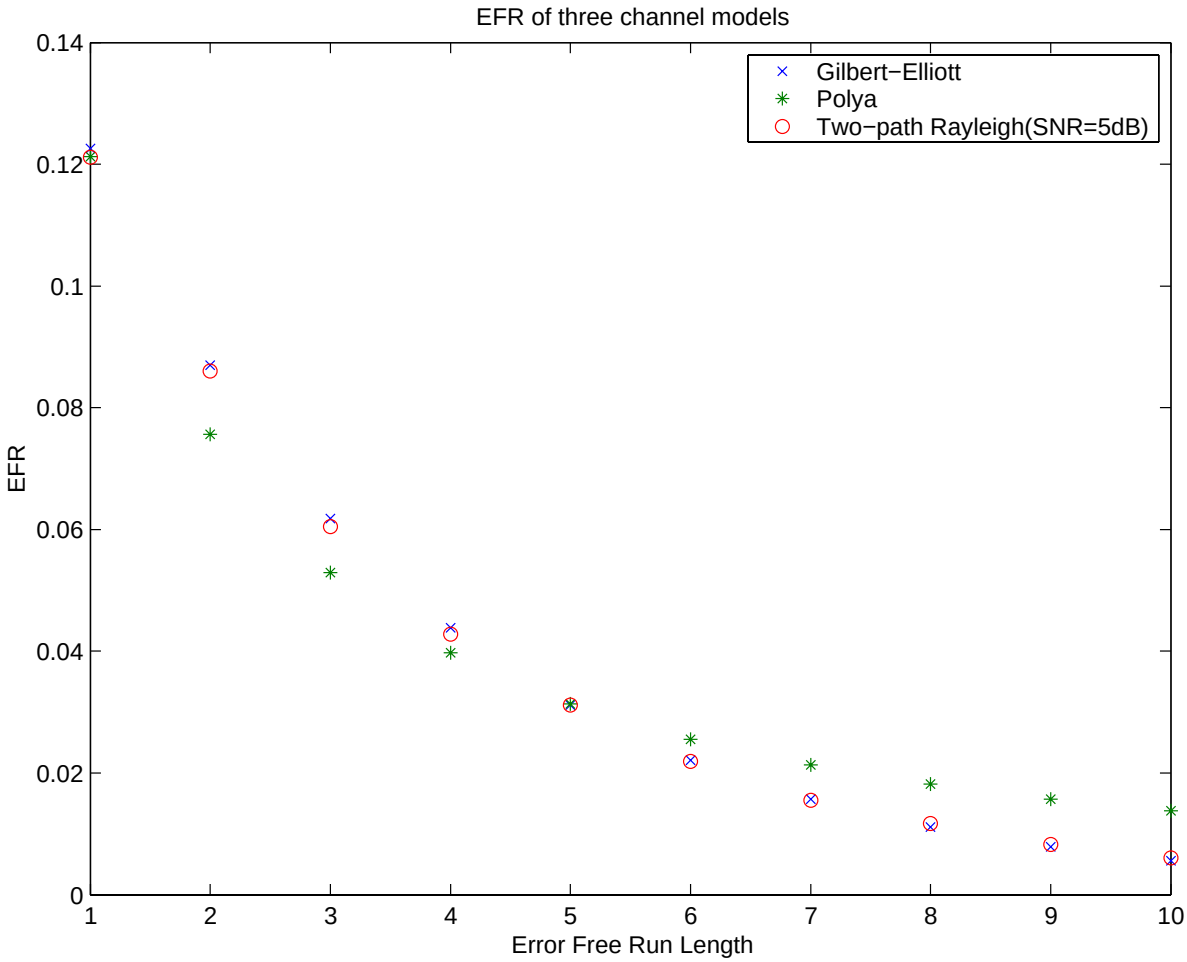

Figure 3.6: The Comparison Between the EFR of Three Models; condition 4

Table 3.5: The Total Difference of EFR Between Models; condition 4

Gilbert vs. Rayleigh	0.006493
Polya vs. Rayleigh	0.052088

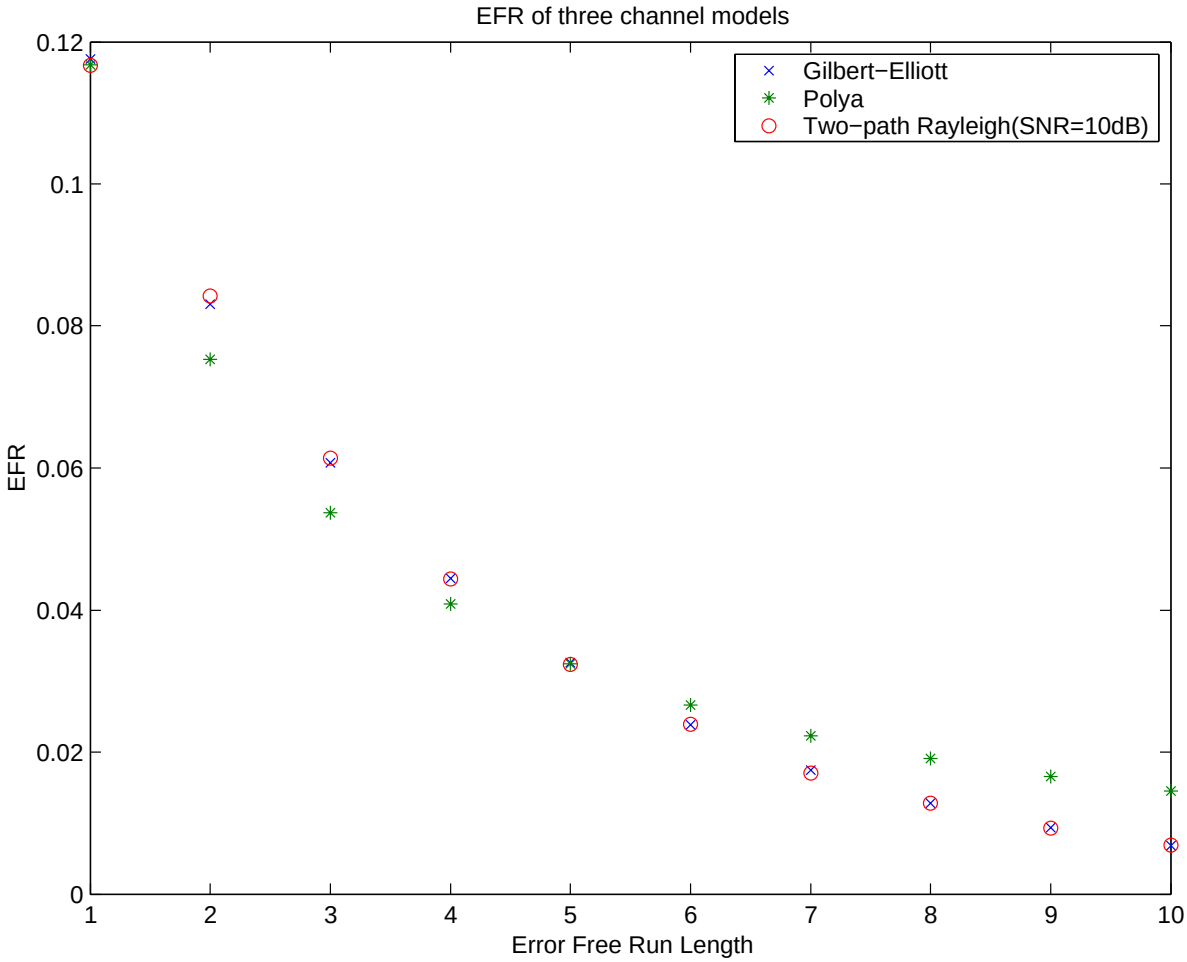

Figure 3.7: The Comparison Between the EFR of Three Models; condition 5

Table 3.6: The Total Difference of EFR Between Models; condition 5

Gilbert vs.Rayleigh	0.003538
Polya vs. Rayleigh	0.049427

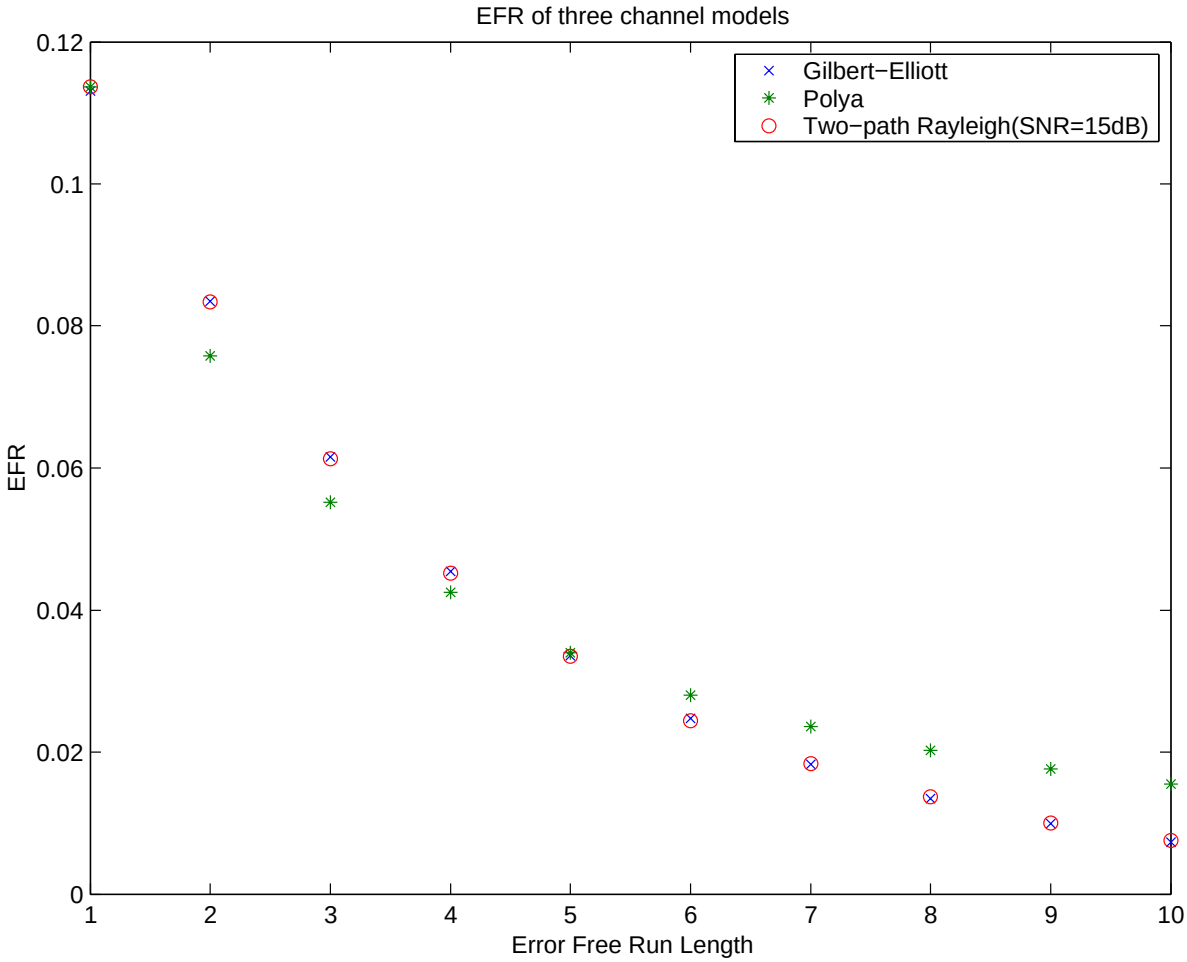

Figure 3.8: The Comparison Between the EFR of Three Models; condition 6

Table 3.7: The Total Difference of EFR Between Models; condition 6

Gilbert vs.Rayleigh	0.002028
Polya vs. Rayleigh	0.04776

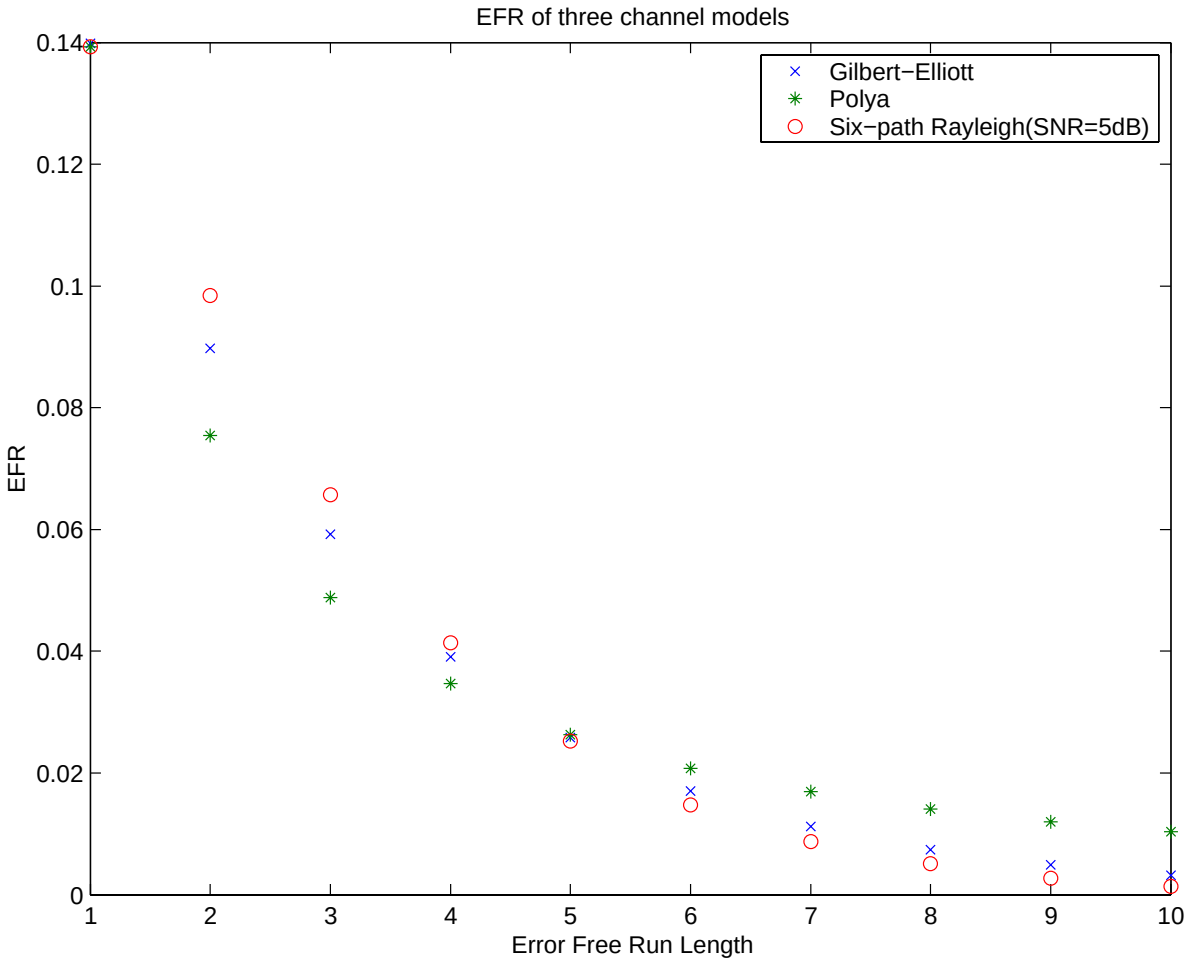

Figure 3.9: The Comparison Between the EFR of Three Models; condition 7

Table 3.8: The Total Difference of EFR Between Models; condition 7

Gilbert vs. Rayleigh	0.029542
Polya vs. Rayleigh	0.088948

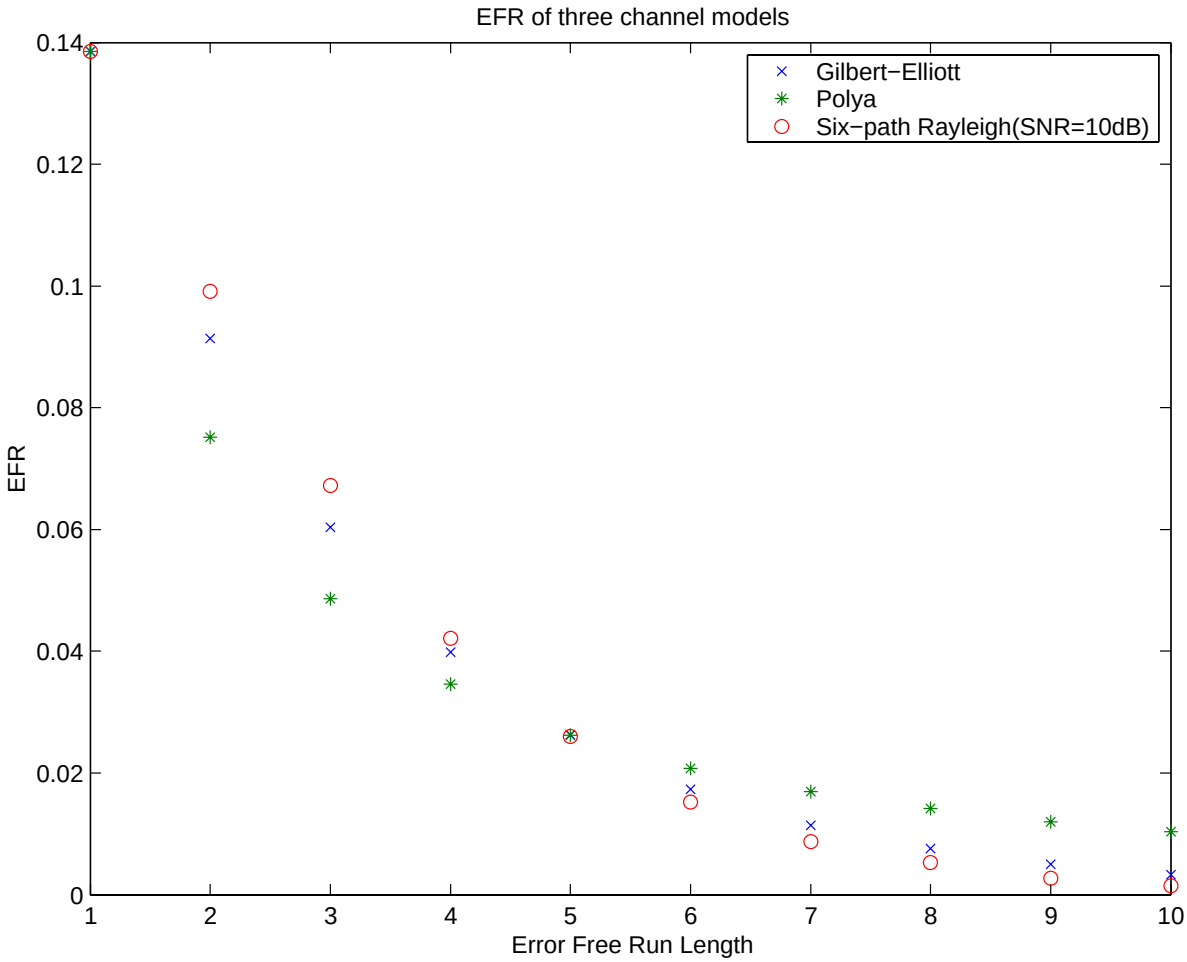

Figure 3.10: The Comparison Between the EFR of Three Models; condition 8

Table 3.9: The Total Difference of EFR Between Models; condition 8

Gilbert vs. Rayleigh	0.028455
Polya vs. Rayleigh	0.091200

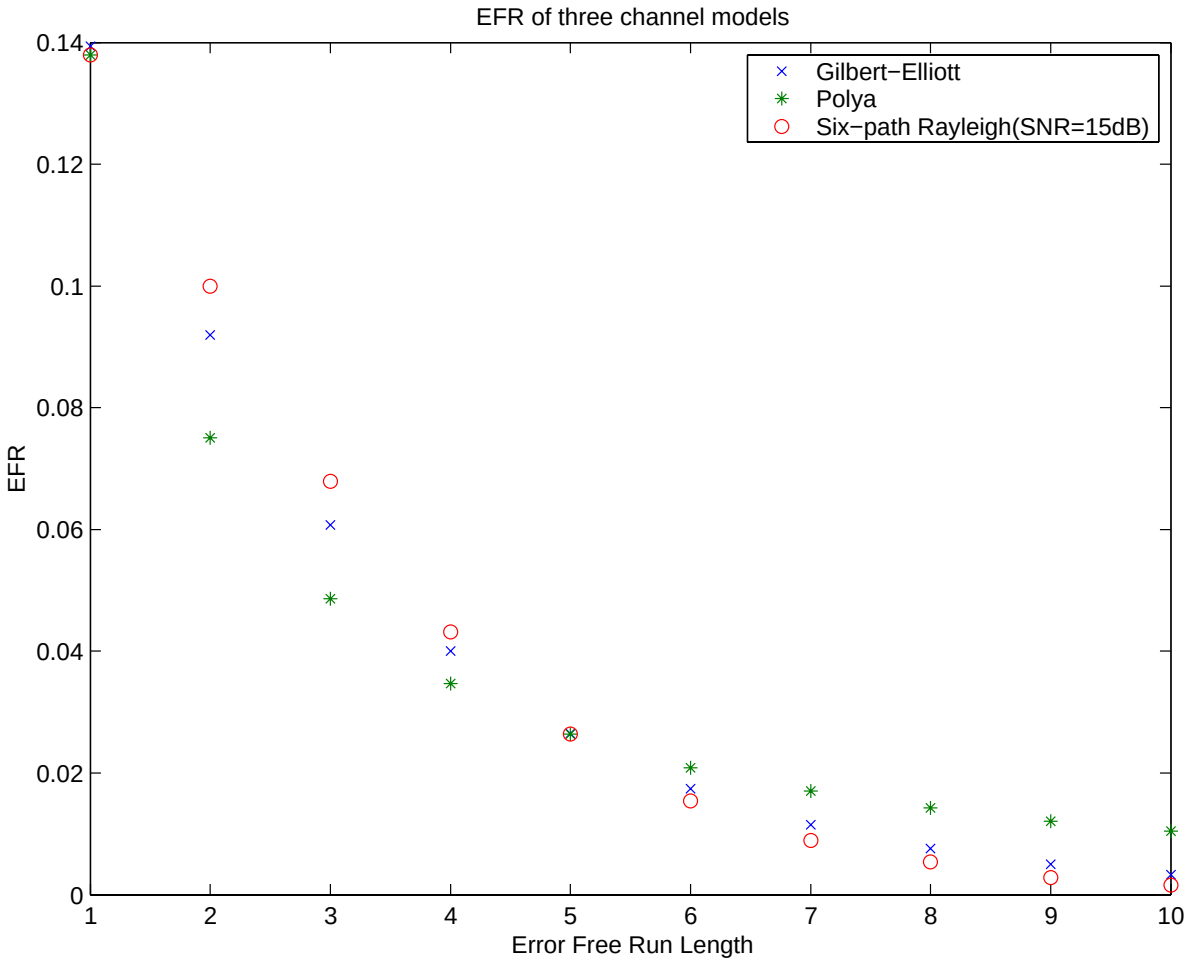

Figure 3.11: The Comparison Between the EFR of Three Models; condition 9

Table 3.10: The Total Difference of EFR Between Models; condition 9

Gilbert vs. Rayleigh	0.030591
Polya vs. Rayleigh	0.093170

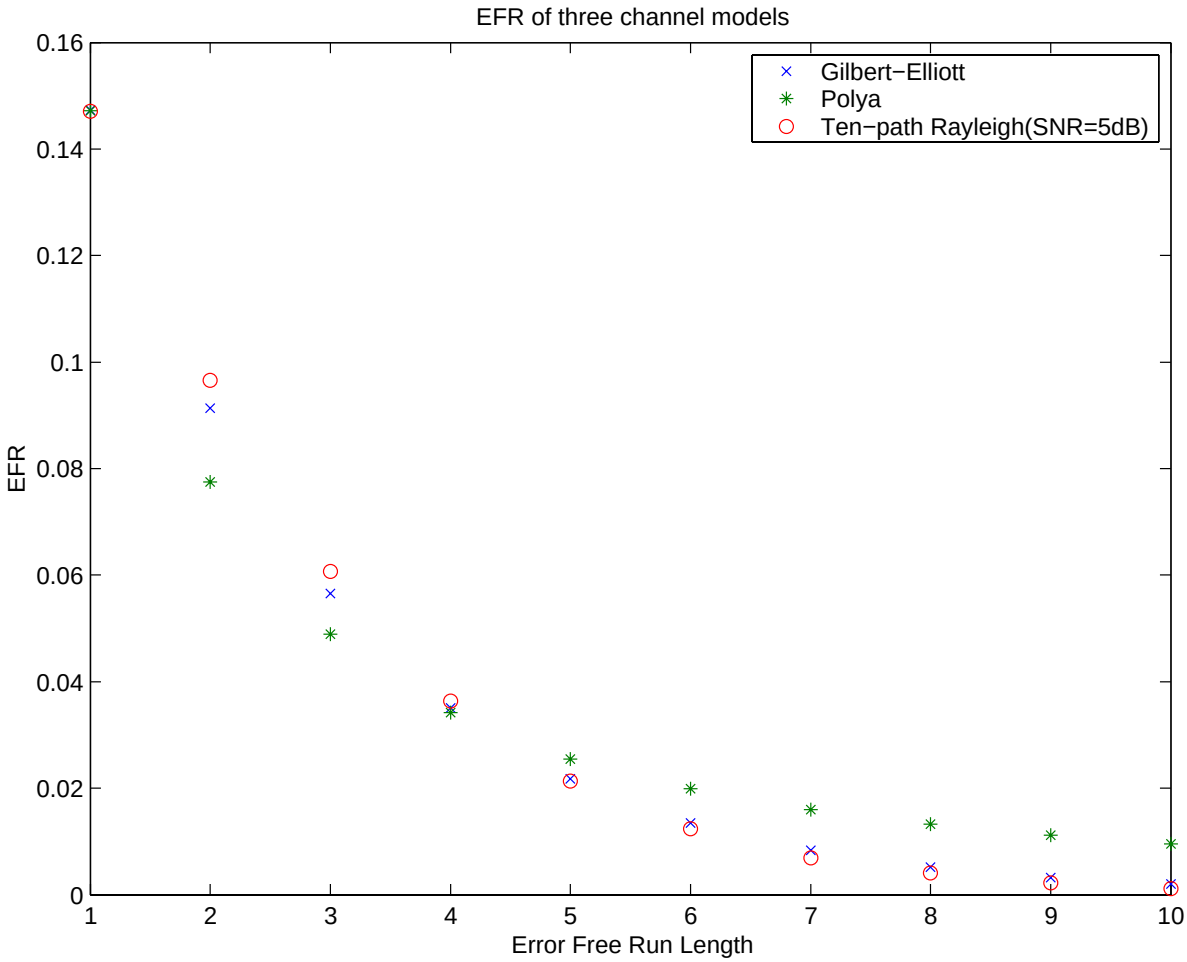

Figure 3.12: The Comparison Between the EFR of Three Models; condition 10

Table 3.11: The Total Difference of EFR Between Models; condition 10

Gilbert vs. Rayleigh	0.016749
Polya vs. Rayleigh	0.080321

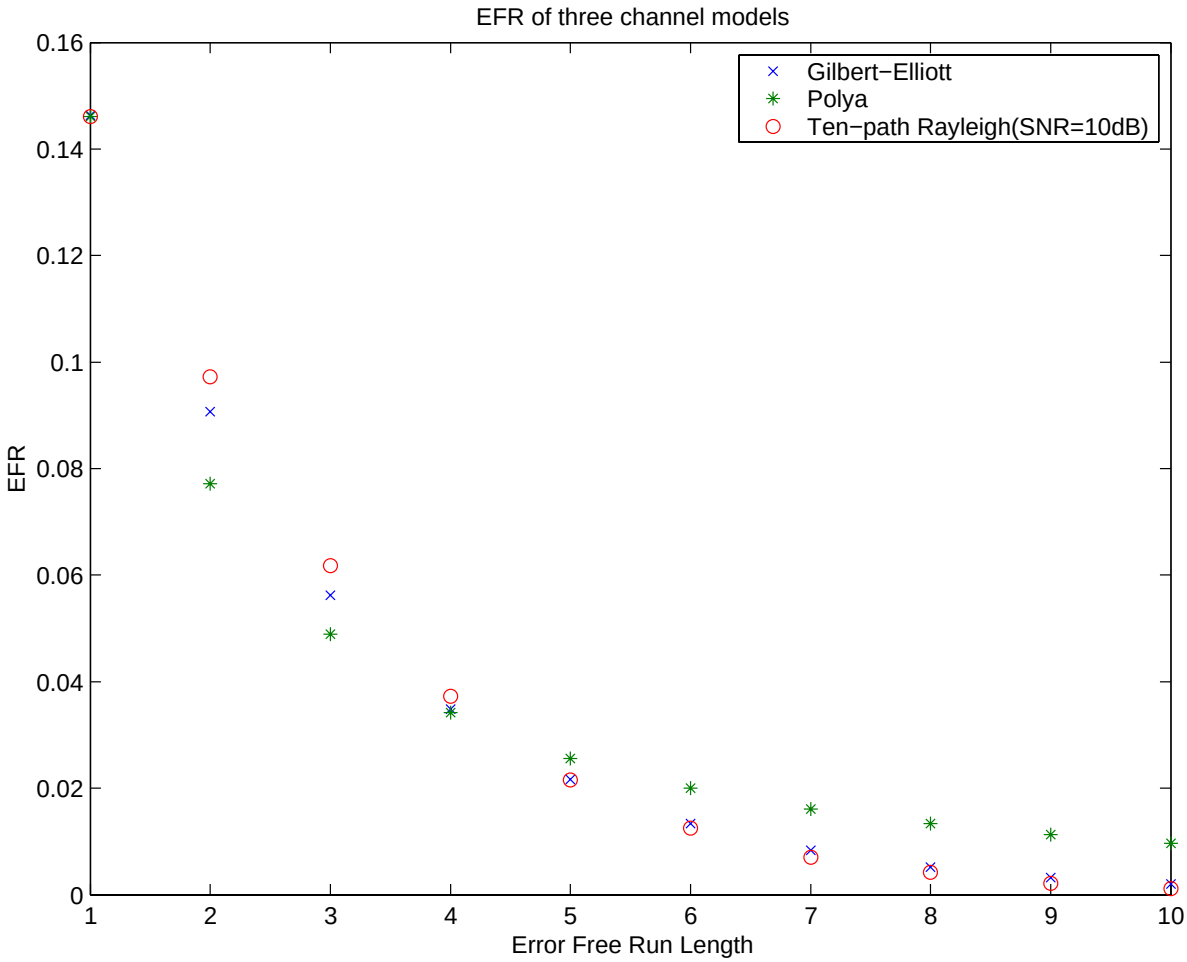

Figure 3.13: The Comparison Between the EFR of Three Models; condition 11

Table 3.12: The Total Difference of EFR Between Models; condition 11

Gilbert vs. Rayleigh	0.019919
Polya vs. Rayleigh	0.083483

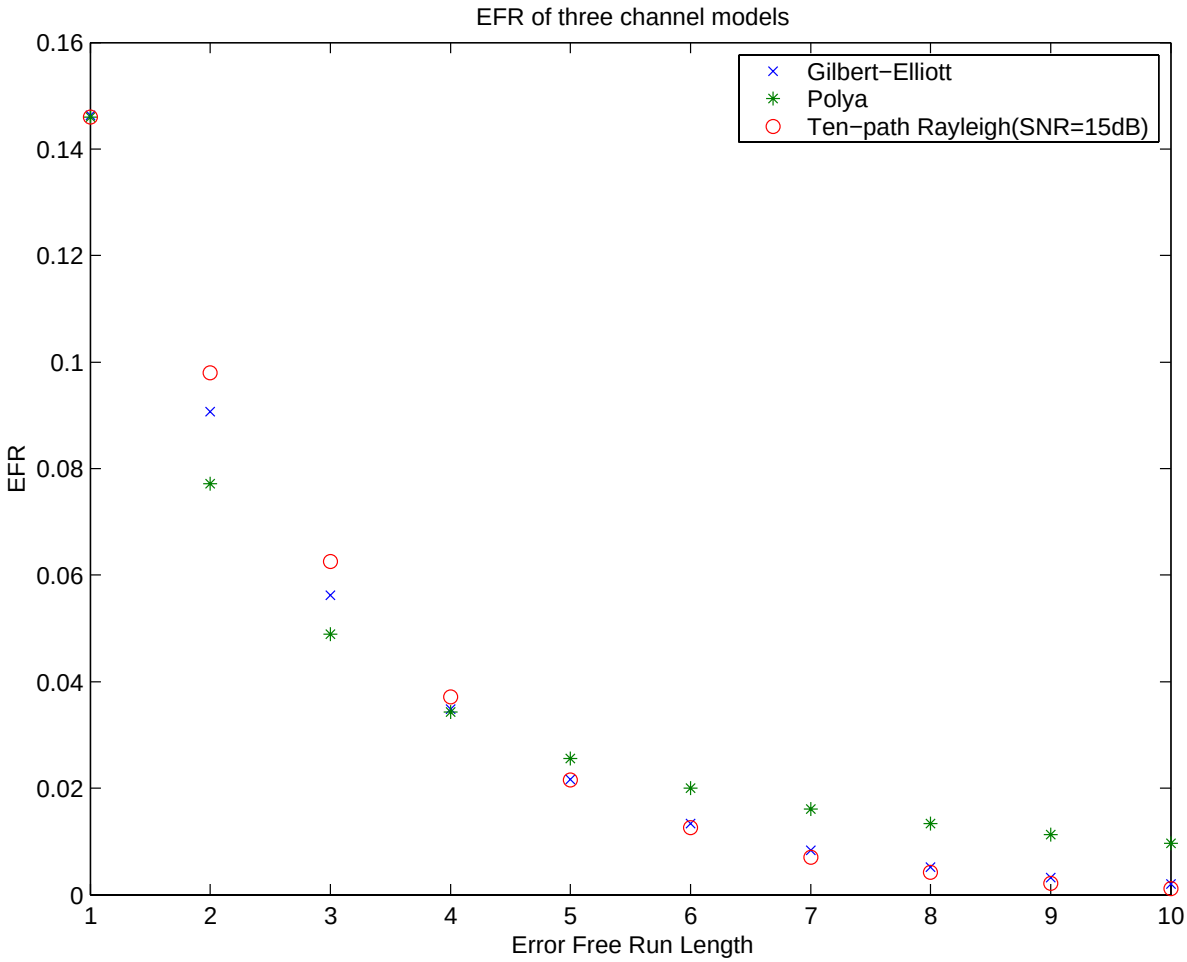

Figure 3.14: The Comparison Between the EFR of Three Models; condition 12

Table 3.13: The Total Difference of EFR Between Models; condition 12

Gilbert vs. Rayleigh	0.021096
Polya vs. Rayleigh	0.084643

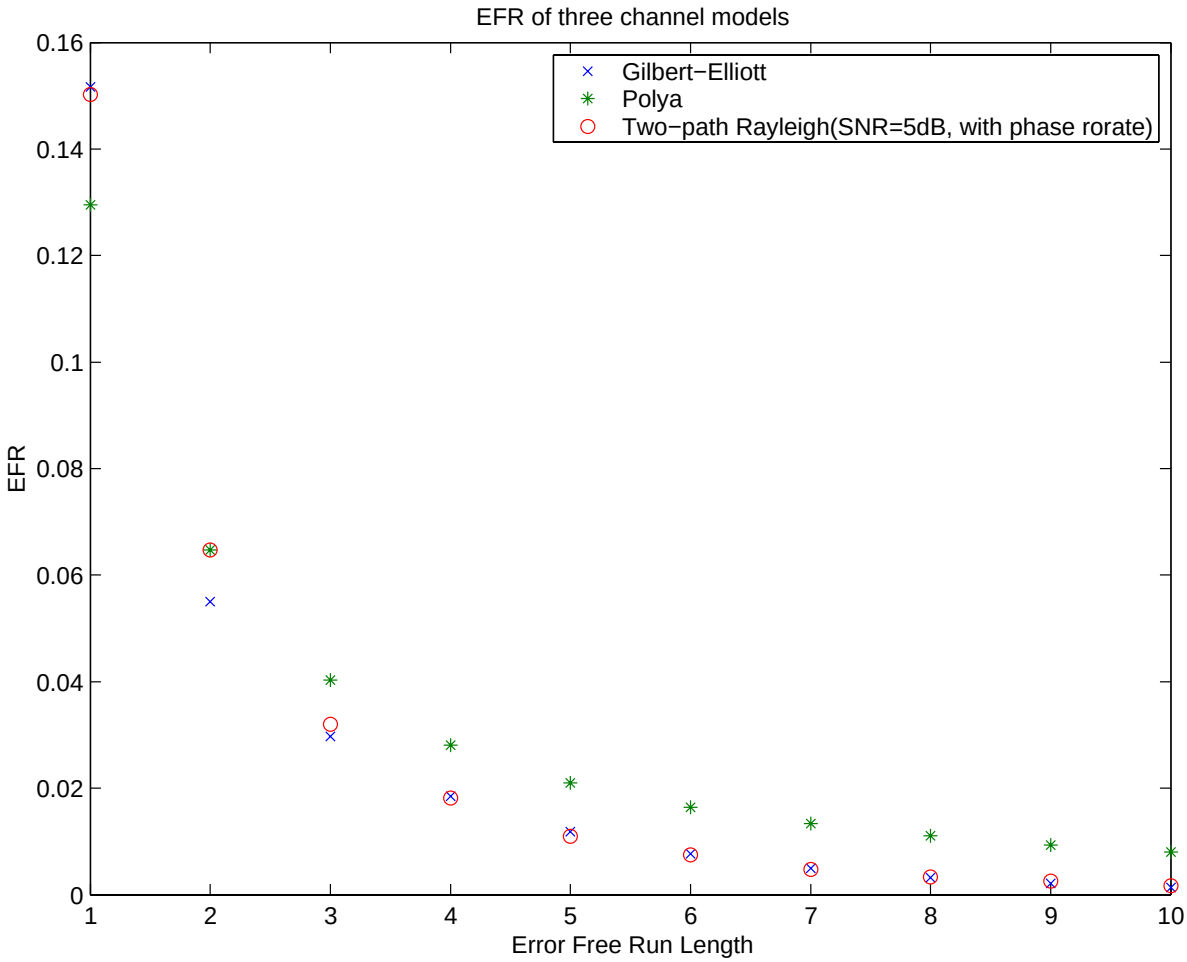

Figure 3.15: The Comparison Between the EFR of Three Models; condition 13

Table 3.14: The Total Difference of EFR Between Models; condition 13

Gilbert vs. Rayleigh	0.015924
Polya vs. Rayleigh	0.087308

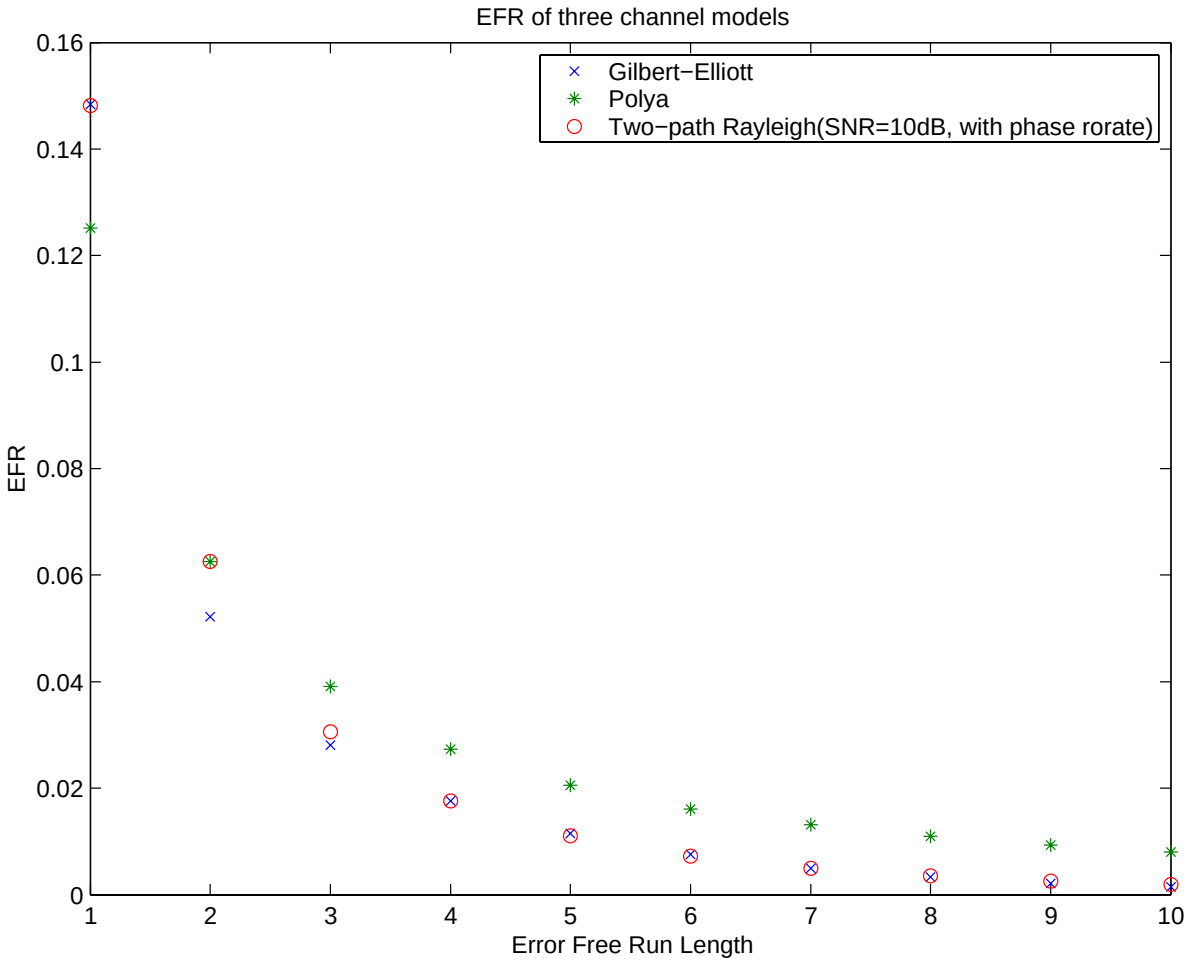

Figure 3.16: The Comparison Between the EFR of Three Models; condition 14

Table 3.15: The Total Difference of EFR Between Models; condition 14

Gilbert vs. Rayleigh	0.015076
Polya vs. Rayleigh	0.088045

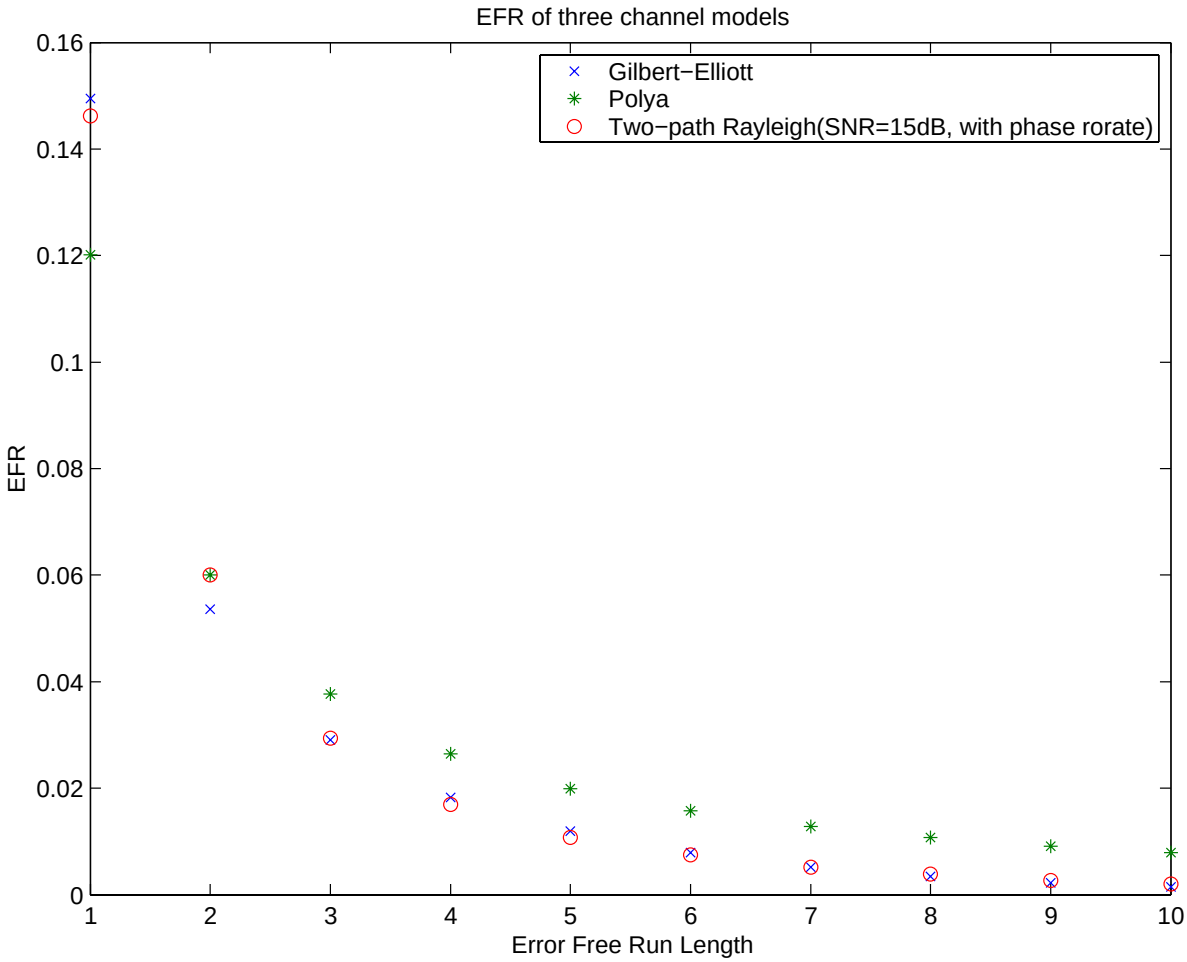

Figure 3.17: The Comparison Between the EFR of Three Models; condition 15

Table 3.16: The Total Difference of EFR Between Models; condition 15

Gilbert vs. Rayleigh	0.014545
Polya vs. Rayleigh	0.088376

Table 3.17: Channel Parameters for Fitting the Rayleigh Channel

Condition	Gilbert (g, b, p_G, p_B)	Polya (R, S, Δ)
1	(0.1, 0.09, 0.24, 0.97)	(820, 2000, 1650)
2	(0.1, 0.09, 0.22, 0.98)	(700, 3500, 1650)
3	(0.11, 0.11, 0.21, 0.98)	(690, 3970, 1650)
4	(0.1, 0.068, 0.29, 1)	(790, 2420, 1700)
5	(0.1, 0.073, 0.268, 0.99)	(690, 2450, 1470)
6	(0.1, 0.071, 0.262, 1)	(662, 2670, 1335)
7	(0.1, 0.065, 0.34, 0.99)	(1005, 1520, 1817)
8	(0.1, 0.062, 0.34, 1)	(991, 1510, 1817)
9	(0.1, 0.061, 0.34, 1)	(979, 1520, 1817)
10	(0.1, 0.06, 0.38, 1)	(1184, 1517, 1817)
11	(0.1, 0.061, 0.38, 1)	(1159, 1511, 1817)
12	(0.1, 0.061, 0.38, 1)	(1156, 1511, 1817)
13	(0.14, 0.34, 0.35, 0.86)	(999, 1000, 1858)
14	(0.14, 0.38, 0.34, 0.86)	(999, 1000, 1994)
15	(0.14, 0.36, 0.34, 0.86)	(999, 1000, 2161)

3.5 Discussion on Simulation Results

According to simulation results shown previously, the EFR of the Gilbert-Elliott model is always closer to that of the Rayleigh fading model than the Polya model. Therefore, from the aspect of EFRs, the Polya model is a weaker representative for the Rayleigh fading channel than the Gilbert-Elliott model. Another interesting observation is that the total difference of EFRs between the Gilbert-Elliott model and two-path Rayleigh fading channel model without phase rotate is particularly small, which hints that the Gilbert-Elliott model is very much suitable for representing a two-path binary-quantized Rayleigh fading channel without phase rotate.

Chapter 4

Conclusions

In this thesis, we examine which of the two channel models, Gilbert-Elliott and Polya, is more suitable to approximate the binary-quantized simplification of a continuous multipath Rayleigh fading channel. Our quest proceeds by means of two different methodologies, an analytical methodology based on divergence, and an empirical methodology based on error free run matching.

Chapter 2 then gives a formal definition of similarity between two channel models in terms of the divergence of channel statistics. According to the definition, similarity between the Polya and the Gilbert-Elliott models is derived under stationarity assumption. The results indicates that at least for one specific case, the Polya channel and the Gilbert-Elliott channel does not resemble to each other. But here, no optimization on the model parameters has been established. There are quite a few future work along this research line.

In Chapter 3, we pre-specifies a targeted multi-path Rayleigh fading channel model. We then test which of the Polya and Gilbert-Elliott channels is a better approximation of the targeted channel based on a quantitative indicator named *error free run* (EFR). The simulation results show that the Polya model is apparently a weaker representative for the Rayleigh fading channel than the Gilbert-Elliott model from the aspect of EFR

matching. Also from the simulations, the two-state Gilbert-Elliott model seems quite suitable to approximate a two-path Rayleigh fading channel without phase rotate.

Bibliography

[1] F. Alajaji and T. Fuja, "A communication channel modeled on contagion," *IEEE Trans. Inform. Theory*, vol. 40, no. 6, pp. 2035–2041, November 1994.

[2] P. Billingsley, *Probability and Measure*. 3rd edition, New York:Wiley, 1995.

[3] T. M. Cover and J. A. Thomas, *Elements of Information Theory*, John Wiley & Sons, Inc.: New York, 1991.

[4] E. O. Elliott, "Estimates of error rates for codes on burst-noise channels," *the Bell System Technical Journal*, pp. 1977–1997, September 1963.

[5] B. D. Fritchman, "A binary channel characterization using partitioned Markov chains," *IEEE Trans. Inform. Theory*, vol. IT-13, no. 2, pp. 221–227, April 1967.

[6] E. N. Gilbert, "Capacity of a burst-noise channel," *the Bell System Technical Journal*, pp. 1253–1265, September 1960.

[7] R. Iordache, I. Tabus, and J. Astola, "Robust index assignment for transmitting vector quantized LSF parameters over finite-memory contagion channels using Hadamard transform," In review, *Circuits, Systems and Signal Processing*, submitted June 2001.

[8] M. Mushkin and I. Bar-David, "Capacity and coding for the Gilbert-Elliott channels," *IEEE Trans. Inform. Theory*, vol. 35, no. 6, pp. 1277–1290, November 1989.

[9] B. O'Hara and A. Petrick, *The IEEE 802.11 Handbook, A Designer's Companion*, IEEE Press, 1999.

[10] J. G. Proakis, *Digital Communications*, 4th edition, McGraw-Hill: New York, 2001.

[11] J. S. Swarts and H. C. Ferreira, "On the evaluation and application of Markov channel models in wireless communication," *Vehicular Technology Conference, 1999. VTC 1999*, vol. 1, pp. 117–121, Fall 1999.